

RESEARCH PAPER



## CSNK1A1/CK1 $\alpha$ suppresses autoimmunity by restraining the CGAS-STING1 signaling

Mingyu Pan<sup>a,b#</sup>, Tongyu Hua<sup>#</sup>, Jiao Lyu<sup>a#</sup>, Yue Yin<sup>a</sup>, Jing Sun<sup>a</sup>, Quanyi Wang<sup>a</sup>, Lingxiao Xu<sup>c,d</sup>, Haiyang Hu<sup>a</sup>, and Chen Wang<sup>a</sup>

<sup>a</sup>State Key Laboratory of Natural Medicines, School of Life Science and Technology, China Pharmaceutical University, Nanjing, Jiangsu, China; <sup>b</sup>Department of Biomedical Science, City University of Hong Kong, Hong Kong, Hong Kong, China; <sup>c</sup>Department of Rheumatology, The affiliated Suqian First People's Hospital of Nanjing Medical University, Suqian, Jiangsu, China; <sup>d</sup>Department of Rheumatology, The First Affiliated Hospital of Nanjing Medical University, Nanjing, Jiangsu, China

### ABSTRACT

STING1 (stimulator of interferon response cGAMP interactor 1) is the quintessential protein in the CGAS-STING1 signaling pathway, crucial for the induction of type I IFN (interferon) production and eliciting innate immunity. Nevertheless, the overactivation or sustained activation of STING1 has been closely associated with the onset of autoimmune disorders. Notably, the majority of these disorders manifest as an upregulated expression of type I interferons and IFN-stimulated genes (ISGs). Hence, strict regulation of STING1 activity is paramount to preserve immune homeostasis. Here, we reported that CSNK1A1/CK1 $\alpha$ , a serine/threonine protein kinase, was essential to prevent the overactivation of STING1-mediated type I IFN signaling through autophagic degradation of STING1. Mechanistically, CSNK1A1 interacted with STING1 upon the CGAS-STING1 pathway activation and promoted STING1 autophagic degradation by enhancing the phosphorylation of SQSTM1/p62 at serine 351 (serine 349 in human), which was critical for SQSTM1-mediated STING1 autophagic degradation. Consistently, SSTC3, a selective CSNK1A1 agonist, significantly attenuated the response of the CGAS-STING1 signaling by promoting STING1 autophagic degradation. Importantly, pharmacological activation of CSNK1A1 using SSTC3 markedly repressed the systemic autoinflammatory responses in the *trex1*<sup>-/-</sup> mouse autoimmune disease model and effectively suppressed the production of IFNs and ISGs in the PBMCs of SLE patients. Taken together, our study reveals a novel regulatory role of CSNK1A1 in the autophagic degradation of STING1 to maintain immune homeostasis. Manipulating CSNK1A1 through SSTC3 might be a potential therapeutic strategy for alleviating STING1-mediated aberrant type I IFNs in autoimmune diseases.

**Abbreviations:** BMDMs: bone marrow-derived macrophages; cGAMP: cyclic GMP-AMP; CGAS: cyclic GMP-AMP synthase; HTDNA: herring testes DNA; IFIT1: interferon induced protein with tetratricopeptide repeats 1; IFNA4: interferon alpha 4; IFNB: interferon beta; IRF3: interferon regulatory factor 3; ISD: interferon stimulatory DNA; ISGs: IFN-stimulated genes; MEFs: mouse embryonic fibroblasts; PBMCs: peripheral blood mononuclear cells; RSAD2: radical S-adenosyl methionine domain containing 2; SLE: systemic lupus erythematosus; STING1: stimulator of interferon response cGAMP interactor 1; TBK1: TANK binding kinase 1.

### ARTICLE HISTORY

Received 25 April 2023  
Revised 22 August 2023  
Accepted 31 August 2023






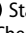


### KEYWORDS

Autoimmunity; autophagy; CSNK1A1; STING1; type I IFN


## Introduction

The CGAS (cyclic GMP-AMP synthase)-STING1 (stimulator of interferon response cGAMP interactor 1) pathway is an essential component of the innate immune system that functions to detect the presence of aberrant cytosolic DNA and triggers the activation of innate immune defense. Upon binding double-stranded DNA (dsDNA), CGAS catalyzes the second messenger cGAMP, which binds to and activates STING1. Acting as a critical adaptor protein, STING1 orchestrates the signal transduction by recruiting TBK1 to trigger IRF3 phosphorylation and induce subsequent type I interferons (IFNs) production, as well as the downstream expression of IFN stimulated genes (ISGs) and other

cytokines [1,2]. Although the IFN response is critical for the host's defense against viruses and other pathogens, chronic IFN activation is tightly associated with the initiation and progression of autoimmune disorders [3,4]. Recent studies reported that undue activation of STING1 was associated with autoinflammatory and autoimmune diseases, including Aicardi-Goutières syndrome (AGS), STING1-associated vasculopathy with onset in infancy (SAVI), and systemic lupus erythematosus (SLE) [5–8]. Thus, a fine-tuned homeostasis of STING1 activity is required to avoid autoimmunity. Understanding the master switches and the regulatory network that restrict the over-activated STING1 will be useful for developing therapeutics against STING1-mediated

**CONTACT** Quanyi Wang  [quanyiwang@cpu.edu.cn](mailto:quanyiwang@cpu.edu.cn)  State Key Laboratory of Natural Medicines, School of Life Science and Technology, China Pharmaceutical University, 639 Longmian Avenue, 210000, Jiangsu, China; Lingxiao Xu  [lingxiao\\_jsph@126.com](mailto:lingxiao_jsph@126.com)  Department of Rheumatology, The affiliated Suqian First People's Hospital of Nanjing Medical University, 223800, Jiangsu, China; Haiyang Hu  [haiyanghu@cpu.edu.cn](mailto:haiyanghu@cpu.edu.cn)  State Key Laboratory of Natural Medicines, School of Life Science and Technology, China Pharmaceutical University, 639 Longmian Avenue, 210000, Jiangsu, China; Chen Wang  [cwang1971@cpu.edu.cn](mailto:cwang1971@cpu.edu.cn)  State Key Laboratory of Natural Medicines, School of Life Science and Technology, China Pharmaceutical University, 639 Longmian Avenue, 210000, Jiangsu, China

<sup>#</sup>These authors contributed equally to this work.

 Supplemental data for this article can be accessed online at <https://doi.org/10.1080/15548627.2023.2256135>

autoimmune diseases. It is well known that STING1 is degraded shortly after the CGAS-STING1 signaling activation, in which the autophagy pathway emerges as a critical mechanism mediating STING1 degradation to avoid its excessive activation [9, 10].

Autophagy is a conserved self-eating process for eliminating intracellular components, damaged organelles, and foreign bodies in eukaryotes [11,12], which is involved in many physiological and pathological processes [13–15]. Recent studies have indicated that autophagy defects are an important trigger in IFN responses, which is associated with SLE disease susceptibility and progression [16]. Many elements of the autophagy system can potentially repress STING1-mediated type I IFN production [17]. For instance, autophagy related 9A (ATG9A) negatively regulates STING1 trafficking from the endoplasmic reticulum (ER) to the Golgi apparatus and inhibits the activation of the TBK1-IRF3-IFN-I axis [18]. Also, STING1 directly interacts with LC3, a ubiquitin-like modifier involved in the formation of autophagosomes, via its LC3-interacting region motifs to mediate its own autophagic degradation to achieve the resolution of immune responses [19]. Besides, the activation of the CGAS-STING1 pathway also leads to SQSTM1-mediated autophagic degradation of STING1 [20]. Although mounting studies have provided evidence for a tight association between the STING1 signaling and autophagy pathway, the detailed regulatory-network underlying STING1 turnover in the autophagy process remains not fully understood.

CSNK1A1 is a serine/threonine protein kinase belonging to the CK1 protein family that is highly conserved in eukaryotes [21,22]. As one of the main components of the WNT-CTNNB1/ $\beta$ -catenin signaling pathway, CSNK1A1 phosphorylates CTNNB1/ $\beta$ -catenin at Ser45 for subsequent BTRC/ $\beta$ -TrCP-mediated ubiquitination and proteasomal degradation [23–25]. In addition, CSNK1A1 acts as a negative regulator of the p53 tumor suppressor by interacting with MDMX to inhibit the DNA-binding and transcriptional activity of p53 [26,27]. CSNK1A1 is also implicated in neurodegenerative diseases [28,29] and multiple cancers [30–32]. However, the physiological function of CSNK1A1 is still largely unknown and needs further exploration.

In this study, we report that CSNK1A1 plays a critical role in negatively regulating the STING1-mediated type I IFN signaling pathway by facilitating the selective autophagic degradation of STING1. Our study revealed that CSNK1A1 interacted with STING1, promoting its autophagic degradation to mitigate over-activation. Mechanistically, CSNK1A1 enhanced phosphorylation of SQSTM1 at the Ser351 site specifically, which lead to selective autophagy of STING1 following the activation of the CGAS-STING1 pathway. Moreover, we observed that SSTC3, a selective CSNK1A1 agonist, inhibited the response of the CGAS-STING1 signaling pathway by promoting STING1's autophagic degradation. Remarkably, SSTC3 suppressed autoinflammatory responses in both *trex1*<sup>-/-</sup> BMDM cells and the *trex1*<sup>-/-</sup> mouse autoimmune disease model. Our research further indicated that activating CSNK1A1 with SSTC3 significantly reduced type

I IFNs and ISGs in the PBMCs of SLE patients, highlighting a promising therapeutic approach for STING1-mediated autoimmune diseases. Overall, our study shed new light on the critical role of CSNK1A1 in regulating the CGAS-STING1 signaling pathway's activity and provides valuable insights into the cross-regulation between the CGAS-STING1 signaling pathway and autophagy.

## Results

### **CSNK1A1 is a novel negative regulator of the CGAS-STING1 signaling pathway**

To test whether CSNK1A1 was participated in DNA-triggered type I IFN signaling, we transfected IFNB luciferase reporter and the internal control renilla luciferase into HEK293 cells, together with an increasing amount of CSNK1A1. Upon HTDNA (herring testes DNA) stimulation, we found that CSNK1A1 significantly inhibited the activation of DNA-triggered type I IFN signaling in a dose-dependent manner, indicating that CSNK1A1 might be involved in regulating the CGAS-STING1 signaling (Figure 1A). To further check this, we performed RNA-seq experiments to measure molecular changes at the gene expression level in CSNK1A1-overexpression and control MEFs (mouse embryonic fibroblasts) after HTDNA stimulation. The result showed that overexpression of CSNK1A1 dramatically downregulated most of the differentially expressed ISGs expression induced by HTDNA (Negative binomial test, FDR < 0.05, Figure S1A). Consistently, the real-time PCR experiments further demonstrated a significant decrease in the expression of two IFN-stimulated genes, *Cxcl10* and *Ifit1*, in the HTDNA treated CSNK1A1-overexpression MEFs (Figure S1B), suggesting a negative role of CSNK1A1 in the regulation of the CGAS-STING1 pathway. To confirm this result, we transfected siRNA to knockdown endogenous CSNK1A1 (Figure 1B) and performed RNA-seq experiments to measure molecular changes at gene expression level in CSNK1A1-knockdown and control MEFs after stimulation of HTDNA. The result showed that silencing CSNK1A1 led to significantly more induction of most of the differentially expressed ISGs (Negative binomial test, FDR < 0.05) compared with that in control MEFs (Figure 1C). We further conducted real-time PCR to validate the expression changes of IRF3-responsive genes (*Ifnb*, *Ifna4*) and IFN-stimulated genes (*Cxcl10*, *Isg15*, *Ifit1*, *Rsad2*). In agreement with the RNA-seq data, there is a marked increase in the expression of *Ifnb*, *Ifna4*, *Cxcl10*, *Isg15*, *Ifit1*, and *Rsad2* in the HTDNA treated CSNK1A1-knockdown MEFs (Figure 1D). TBK1 and IRF3 phosphorylation is a hallmark of the CGAS-STING1 signaling pathway [33]. Compared to that in control MEFs, TBK1 and IRF3 phosphorylation triggered by HTDNA was enhanced in CSNK1A1-knockdown MEFs (Figure 1E). In addition, the expression of IRF3-responsive genes and ISGs triggered by cGAMP, a ligand that specifically activates the CGAS-STING1 signaling [34], was also markedly increased in CSNK1A1-knockdown MEFs (Figure 1F). Also, TBK1 and IRF3 phosphorylation triggered by cGAMP was enhanced in CSNK1A1-knockdown MEFs (Figure 1G). Taken together, these data

indicated that CSNK1A1 is a novel negative regulator of the CGAS-STING1 signaling pathway.

### **The kinase activity of CSNK1A1 is required for repressing the CGAS-STING1 signaling**

Given that CSNK1A1 is a serine/threonine protein kinase, we next explored whether its effect on the regulation of the CGAS-STING1 signaling pathway was dependent on its kinase activity. To check this, we constructed a CSNK1A1 R186G (arginine mutated to glycine at position 186) and K232G mutant (lysine mutated to glycine at position 232), which lacked kinase activity [35]. Ectopic expression of wild-type CSNK1A1 suppressed HTDNA induced IFN and ISGs gene expression in MEFs (Figure S1A-B). In contrast, ectopic expression of the CSNK1A1 mutant failed to exert the same effect (Figure 2A-C). In addition, the CSNK1A1 mutant did not inhibit the HTDNA or cGAMP induced IFNB-luciferase expression (Figure 2B-D). Also, the CSNK1A1 mutant failed to attenuate HTDNA or cGAMP induced TBK1 and IRF3 phosphorylation (Figure 2E,F). Collectively, these results indicate that the kinase activity of CSNK1A1 is indispensable for regulating the CGAS-STING1 signaling pathway.

### **CSNK1A1 interacts with STING1 and targets STING1 for degradation**

To explore how CSNK1A1 regulates the activity of the CGAS-STING1 signaling, we overexpressed an increasing amount of CSNK1A1 and CGAS, STING1, TBK1, or IRF3 5D (a persistently active form of IRF3) [9], together with IFNB-luciferase reporter in HEK293 cells. Previous studies reported that overexpression of each gene of the CGAS-STING1-TBK1-IRF3 axis strongly activates the CGAS-STING1 signaling and leads to IFNB induction [9]. Therefore, manipulation of CSNK1A1 expression together with the overexpression of CGAS, STING1, TBK1, or IRF3 5D could determine more specific signaling conduction events regulated by CSNK1A1. The result showed that CSNK1A1 inhibited type I IFN signaling induced by CGAS and STING1 but not by TBK1 or IRF3 5D (Figure 3A). In addition, CSNK1A1 dramatically affected cGAMP-induced activation of IRF3-responsive genes (Figures 1F and 2C-F). Since CGAS and TBK1 act in the upstream and downstream of STING1 in the signaling transduction axis of the CGAS-STING1 signaling, respectively [6], these data suggested that CSNK1A1 regulated the CGAS-STING1 signaling mediated type I IFN signaling at STING1 level. We further investigated whether the regulation of CSNK1A1 on STING1 was through their interaction. Co-immunoprecipitation and immunoblot analysis revealed that CSNK1A1 was specifically associated with STING1, whereas CSNK1A1 did not interact with CGAS, TBK1, or IRF3 (Figure 3B). Consistent with this data, immunofluorescence imaging revealed that the colocalization of CSNK1A1 and STING1 was enhanced in the stimulation of HTDNA (Figure 3C). Taken together, these data demonstrated that CSNK1A1 interacts with STING1.

We next sought to investigate the precise molecular mechanism underlying CSNK1A1-attenuated type I IFN signaling by targeting STING1. Previous studies found that

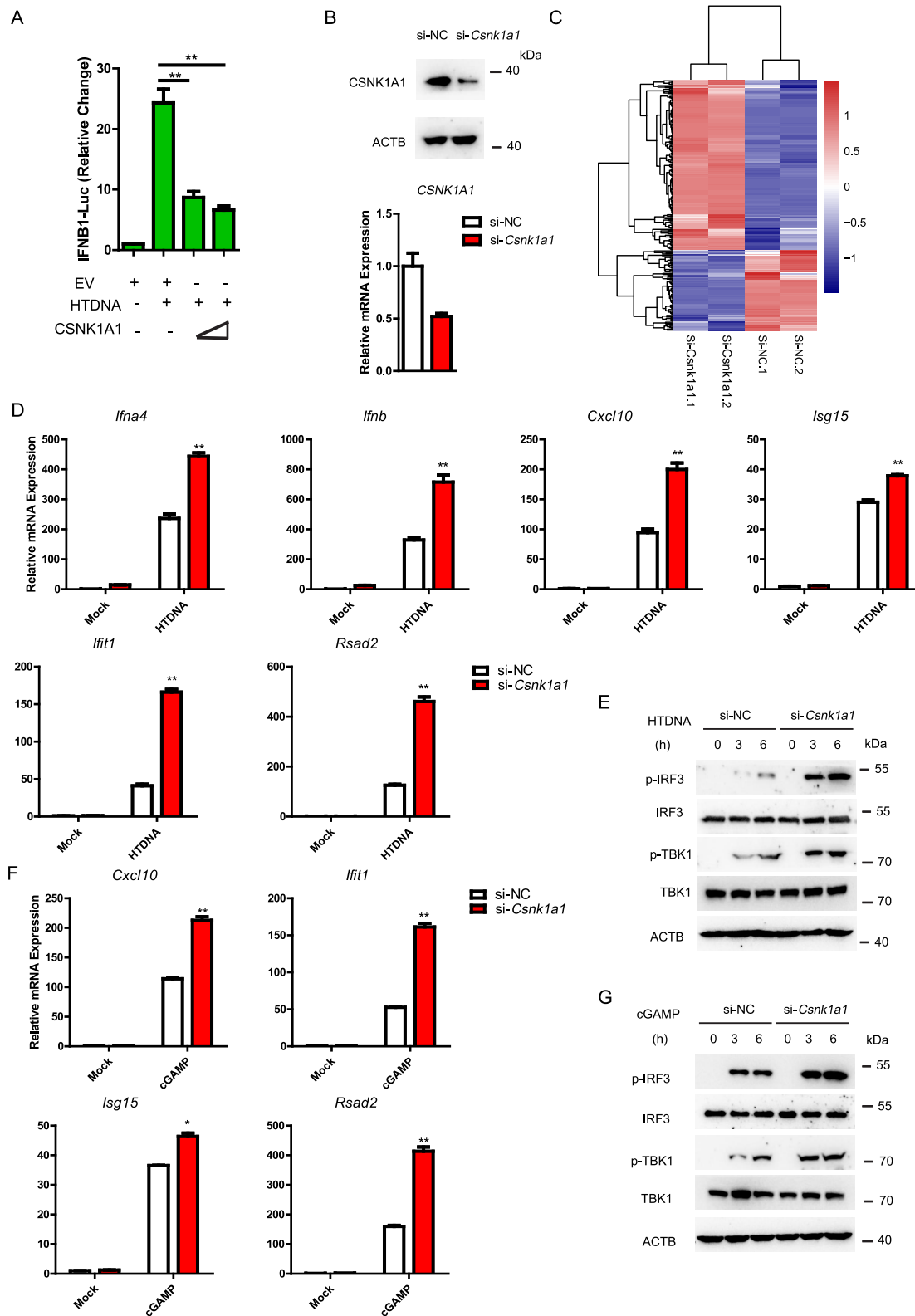
STING1 degradation occurs shortly after the CGAS-STING1 signaling activation [19]. We found that the overexpression of CSNK1A1 resulted in accelerated degradation of STING1 after HTDNA stimulation (Figure 3D). Similar results were observed when IFN stimulatory DNA (ISD) and cGAMP were used as stimuli (Figure 3E,F). To further confirm these results, we examined the protein level of STING1 in CSNK1A1-knockdown cells after HTDNA or cGAMP stimulation and found that the knockdown of CSNK1A1 attenuated the degradation of STING1 (Figure 3G). In addition, the overexpression of CSNK1A1 mutant failed to promote STING1 degradation after HTDNA or cGAMP stimulations (Figure 3I,J). Collectively, these data suggested that CSNK1A1 suppresses type I IFN signaling by promoting the degradation of STING1, which is dependent on its kinase activity.

### **CSNK1A1 promotes the degradation of STING1 through autophagy**

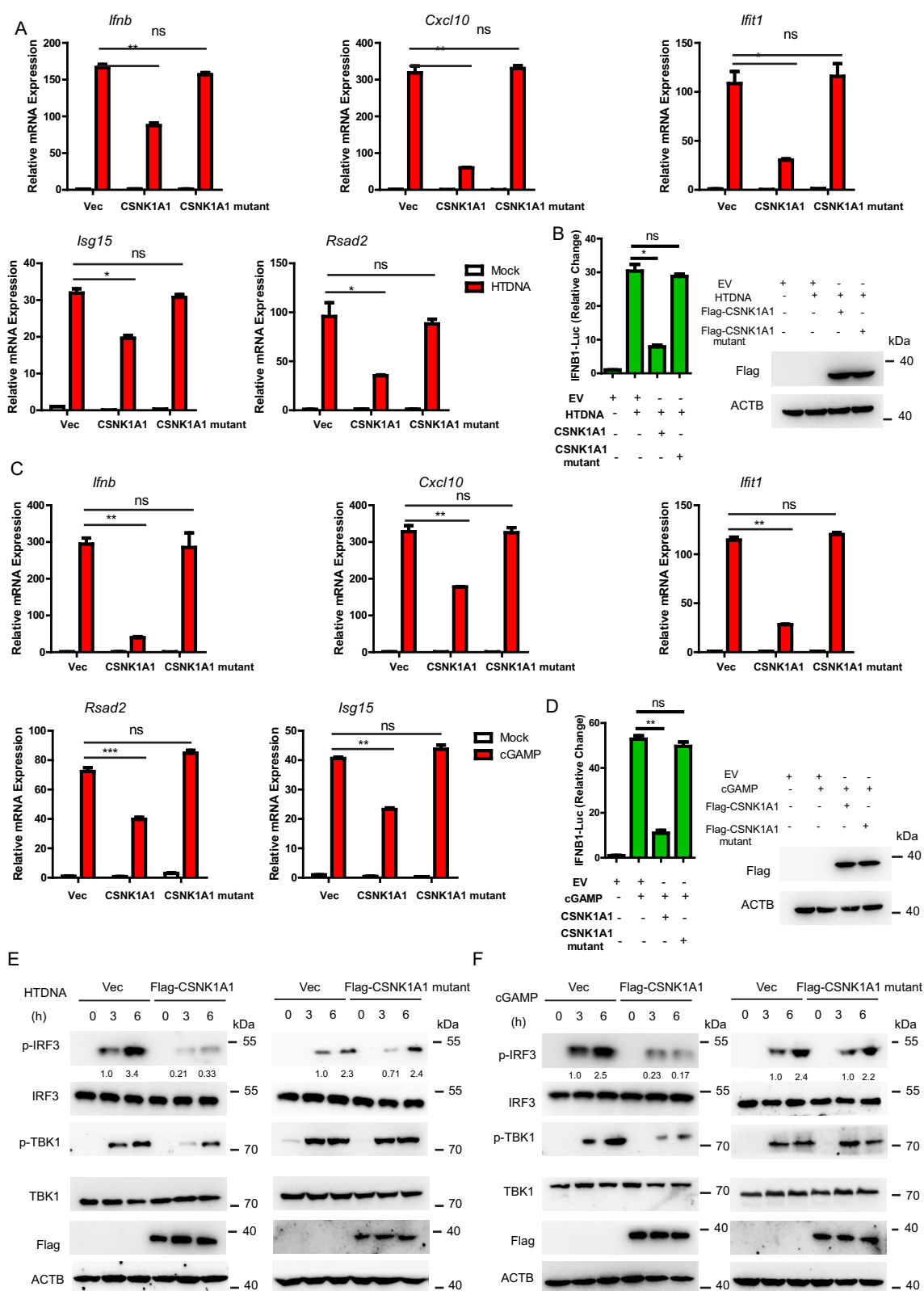
In eukaryotic cells, the ubiquitin-proteasome system (UPS) and the autophagy-lysosome pathway are the two main protein degradation pathways [36, 37]. We further explored which of the two pathways might be involved in CSNK1A1 mediated STING1 degradation. We observed that the overexpression of CSNK1A1 mediated downregulation of STING1 protein abundance was rescued by the treatments with the autophagy inhibitor Baf A1 and chloroquine, but not the proteasome inhibitor MG132 (Figure 4A-C), indicating that CSNK1A1 promoted the degradation of STING1 through autophagy. To verify this, we further explored the effect of CSNK1A1 in autophagic flux by determining the lipidation of LC3, a well-characterized autophagy hallmark [38]. The result showed that LC3-II was decreased in CSNK1A1-knockdown cells and increased in CSNK1A1-overexpression cells, which suggested that CSNK1A1 enhanced autophagic activity (Figure 4D,E). Also, immunofluorescence analysis further confirmed that CSNK1A1 knockdown reduced the colocalization between STING1 and LC3B (Figure 4F). We further assessed the function of CSNK1A1 in ATG5 knockdown MEF cells, in which autophagy is impaired [39]. We found that the abundance of STING1 in ATG5 knockdown cells was largely not affected by the overexpression of CSNK1A1 (Figure 4G). Additionally, CSNK1A1-mediated IFN signaling suppression was abolished in autophagy inhibited cells (Figure 4H). Together, these results indicated that CSNK1A1 promotes STING1 degradation via autophagy, which in turn suppresses STING1-mediated type I IFN signaling.

### **CSNK1A1 accelerates STING1 autophagic degradation by promoting the phosphorylation of SQSTM1 at Ser351**

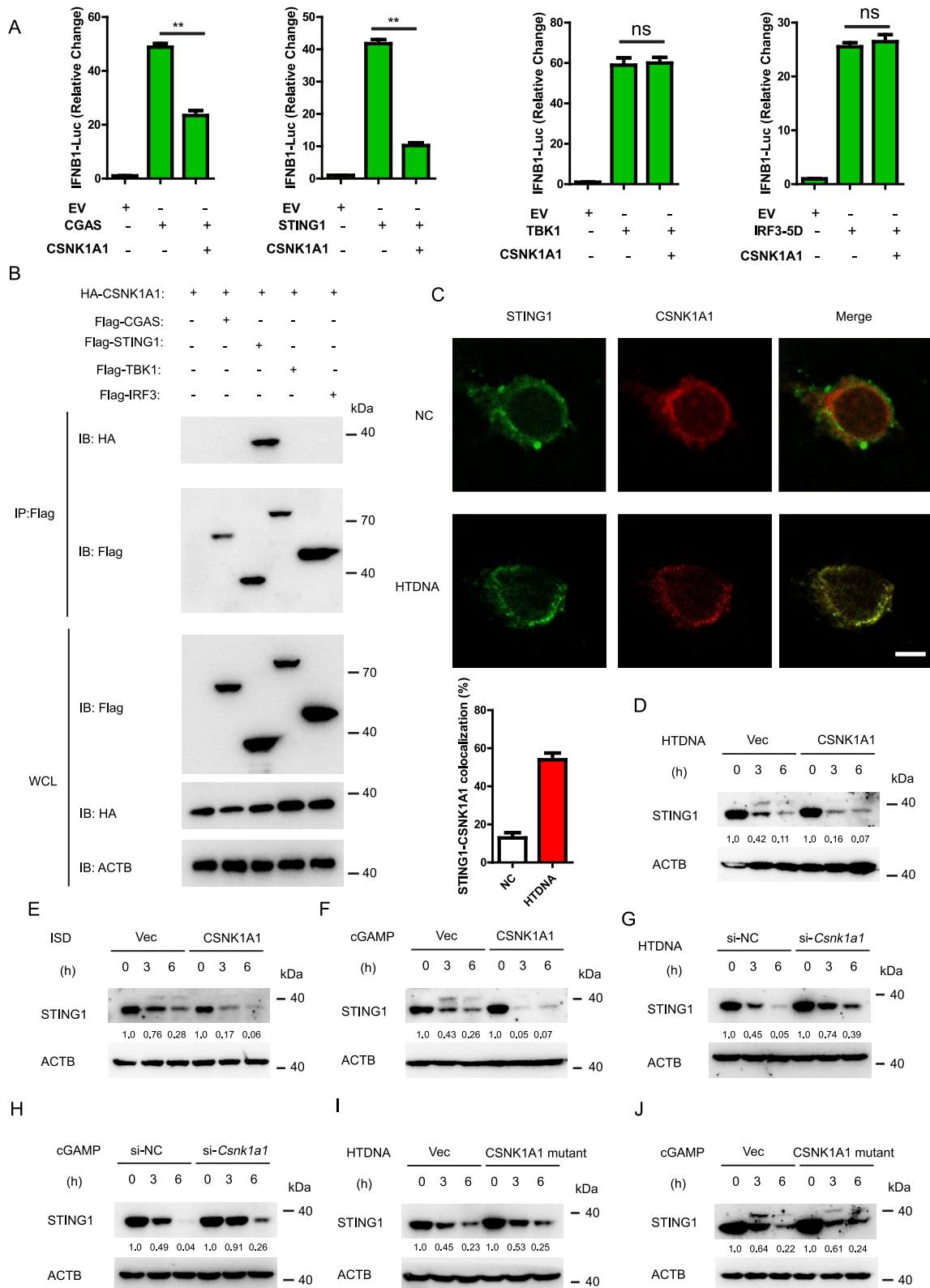
We went on to investigate how CSNK1A1 regulates STING1 autophagic degradation. A previous study reported that the autophagy receptor SQSTM1 is an essential factor in mediating STING1 autophagic degradation by interacting with STING1 [20]. We found CSNK1A1 promoted the phosphorylation of SQSTM1 at Ser351 (Ser349 in human) after



**Figure 1.** CSNK1A1 is a novel regulator of the CGAS-STING1 signaling pathway. (A) Luciferase activity in HEK293 cells transfected with an IFN $\beta$  luciferase reporter, together with an empty vector or increasing amount of plasmid expressing CSNK1A1, activated by HTDNA. The firefly- and renilla luciferase signals were detected with Dual Glo<sup>®</sup> luciferase assay (Promega). (B) MEF cells were transfected with the indicated siRNAs. Cell lysates were collected for western blot analysis of CSNK1A1 and ACTB. Also, CSNK1A1 mRNAs were measured by real-time PCR. (C) The heatmap of expression changes of differentially expressed ISGs between negative control (NC) or *Csnk1a1* siRNAs transfected MEFs stimulated with HTDNA (2  $\mu$ g per well) for 3 h. For each gene, the expression level was normalized (Z-score) across samples. (D) MEFs transfected negative control (NC) or *Csnk1a1* siRNAs were stimulated with HTDNA (2  $\mu$ g per well) for 3 h. Then, the induction of *Ilnb*, *Ilna4*, *Cxcl10*, *Isg15*, *Ifit1*, and *Rsad2* mRNAs was measured by real-time PCR. (E) MEFs transfected negative control (NC) or *Csnk1a1* siRNAs were stimulated with HTDNA for 0, 3, 6 h, respectively. Then, cell lysates were collected for western blot analysis of indicated protein. (F) MEFs transfected negative control (NC) or *Csnk1a1* siRNAs were stimulated with cGAMP (1  $\mu$ g per well) for 3 h. Then, the induction of *Cxcl10*, *Isg15*, *Ifit1*, and *Rsad2* mRNAs was measured by real-time PCR. (G) MEFs transfected negative control (NC) or *Csnk1a1* siRNAs were stimulated with cGAMP for 0, 3, 6 h, respectively. Then, cell lysates were collected for western blot analysis of indicated protein. Graphs show the mean  $\pm$  SEM, and the data shown are representative of three independent experiments. \* $p < 0.05$ ; \*\* $p < 0.01$ ; \*\*\* $p < 0.001$  (two-tailed t-test).



**Figure 2.** CSNK1A1 represses the CGAS-STING1 signaling responses and functions dependently its kinase activity. (A) MEFs transfected control vectors (Vec) or CSNK1A1 expression plasmids (CSNK1A1) or CSNK1A1 mutant expression plasmids (CSNK1A1 mutant) were stimulated with HTDNA (2  $\mu$ g per well) for 3 h. Then, the induction of *Ifnb*, *Cxcl10*, *Isg15*, *Ifit1*, and *Rsad2* mRNAs was measured by real-time PCR. (B) luciferase activity in HEK293 cells transfected with an IFN $\beta$  luciferase reporter, together with an empty vector or increasing amount of plasmid expressing CSNK1A1 or CSNK1A1 mutant, activated by HTDNA. The firefly- and renilla luciferase signals were detected with Dual Glo<sup>®</sup> luciferase assay (Promega). (C) MEFs transfected control vectors (Vec) or CSNK1A1 expression plasmids (CSNK1A1) or CSNK1A1 mutant expression plasmids (CSNK1A1 mutant) were stimulated with cGAMP (1  $\mu$ g per well) for 3 h. Then, the induction of *Ifnb*, *Cxcl10*, *Isg15*, *Ifit1*, and *Rsad2* mRNAs was measured by real-time PCR. (D) luciferase activity in HEK293 cells transfected with an IFN $\beta$  luciferase reporter, together with an empty vector or increasing amount of plasmid expressing CSNK1A1 or CSNK1A1 mutant, activated by cGAMP. The firefly- and renilla luciferase signals were detected with Dual Glo<sup>®</sup> luciferase assay (Promega). (E) MEFs transfected control vectors (Vec) or CSNK1A1 expression plasmids (CSNK1A1) or CSNK1A1 mutant expression plasmids (CSNK1A1 mutant) were stimulated with HTDNA for 0, 3, 6 h, respectively. Then, cell lysates were collected for western blot analysis of indicated protein. (F) MEFs transfected control vectors (Vec) or CSNK1A1 expression plasmids (CSNK1A1) or CSNK1A1 mutant expression plasmids (CSNK1A1 mutant) were stimulated with cGAMP for 0, 3, 6 h, respectively. Then, cell lysates were collected for western blot analysis of indicated protein. Graphs show the mean  $\pm$  SEM, and the data shown are representative of three independent experiments. \* $p$  < 0.05; \*\* $p$  < 0.01; \*\*\* $p$  < 0.001 (two-tailed t-test).



**Figure 3.** CSNK1A1 interacts STING1 and targets STING1 for degradation. (A) luciferase activity in HEK293 cells transfected with an IFNβ luciferase reporter, together with an empty vector or increasing amount of plasmid expressing CSNK1A1, activated by CGAS, STING1, TBK1 or IRF3 5D. The firefly- and renilla luciferase signals were detected with Dual Glo<sup>®</sup> luciferase assay (Promega). (B) HEK293T cells were transfected with the indicated plasmids. Then, cell lysates were immunoprecipitated with an anti-flag antibody and then immunoblotted with the indicated antibodies. (C) MEFs were stimulated with HTDNA for 3 h, then stained with the indicated antibodies before imaging by confocal microscopy. Scale bars: 10 μm. (D) MEFs transfected control vectors (Vec) or CSNK1A1 expression plasmids (CSNK1A1) were stimulated with HTDNA (2 μg per well) for 0, 3, 6 h respectively. Then, Cell lysates were collected for western blot analysis of STING1 and ACTB. (E) MEFs transfected control vectors (Vec) or CSNK1A1 expression plasmids (CSNK1A1) were stimulated with ISD (2 μg per well) for 0, 3, 6 h respectively. Then, Cell lysates were collected for western blot analysis of STING1 and ACTB. (F) MEFs transfected control vectors (Vec) or CSNK1A1 expression plasmids (CSNK1A1) were stimulated with cGAMP (1 μg per well) for 0, 3, 6 h respectively. Then, Cell lysates were collected for western blot analysis of STING1 and ACTB. (G) MEFs transfected negative control (NC) or *Csnk1a1* siRnas were stimulated with HTDNA (2 μg per well) for 0, 3, 6 h respectively. Then, Cell lysates were collected for western blot analysis of STING1 and ACTB. (H) MEFs transfected negative control (NC) or *Csnk1a1* siRnas were stimulated with cGAMP (1 μg per well) for 0, 3, 6 h respectively. Then, Cell lysates were collected

HTDNA or cGAMP stimulation but not the phosphorylation of SQSTM1 at Ser405 (Ser403 in human) (Figure 5A,B). Further, we detected the interaction between CSNK1A1 and SQSTM1 through Co-immunoprecipitation and immunoblot analysis by co-expressing these two molecules in HEK293T cells (Figure 5C). Also, Co-immunoprecipitation and immunoblot analyses revealed that CSNK1A1 interacted with SQSTM1 after HTDNA or cGAMP treatment in MEF cells (Figure 5D,E). Furthermore, the proximity ligation assay result confirmed the interaction between CSNK1A1 and SQSTM1 after HTDNA stimulation (Figure 5F). In addition, we found CSNK1A1 failed to inhibit HTDNA or cGAMP induced IFNB and ISGs expression in SQSTM1-deficient MEFs (Figure 5G, Figure S2A). Collectively, these data demonstrated that CSNK1A1 interacts with SQSTM1 and promotes the phosphorylation of SQSTM1 at Ser351 after the CGAS-STING1 signaling activation.

To further investigate the role of S351-phosphorylated SQSTM1 in STING1 autophagic degradation, we constructed two SQSTM1 mutant expression plasmids, including nonphosphorylated mutant SQSTM1<sup>S351A</sup> (serine mutated to alanine at position 351) and phospho-mimic mutant SQSTM1<sup>S351E</sup> (serine mutated to glutamic acid at position 351) [40]. We observed that the turnover of STING1 was abolished in SQSTM1-deficient MEFs, and reconstitution of WT SQSTM1 expression in SQSTM1-deficient MEFs enabled these cells to degrade STING1 after CGAS-STING1 signaling activation (Figure 5H), which was in line with previous observations [20]. Further, the reconstitution of SQSTM1<sup>S351A</sup> expression significantly attenuated STING1 degradation compared to WT SQSTM1 (Figure 5I). In contrast, the reconstitution of SQSTM1<sup>S351E</sup> expression dramatically promoted STING1 degradation compared to WT SQSTM1 (Figure 5J), which indicated that S351-phosphorylated SQSTM1 is important for mediating STING1 degradation. Previous study showed the phosphorylation of SQSTM1 at Ser405 was essential to regulate STING1 autophagic degradation [20]. We found the mutation of SQSTM1 at ser351 dampened but not abolished SQSTM1-mediated STING1 degradation (Figure 5I). To test whether the effects of SQSTM1 phosphorylation at Ser351 and Ser405 on STING1 degradation are mutually exclusive, we constructed a SQSTM1 mutant expression plasmid by mutating both sites (SQSTM1<sup>S405A,S351A</sup>, serine mutated to alanine at position 351 and 405). The results showed that the reconstitution of SQSTM1<sup>S405A,S351A</sup> expression almost completely abolished STING1 degradation compared to WT SQSTM1 (Figure S2B), indicating that the phosphorylation at Ser351 and Ser405 both participated in SQSTM1-mediated STING1 degradation. Also, we observed that the two phosphorylation sites did not affect phosphorylation of the other (Figure S2C-D). In addition, we transfected WT SQSTM1 and SQSTM1<sup>S351A</sup> expression plasmids into SQSTM1-knockout MEFs and found that the interaction between SQSTM1 and STING1 was significantly impaired in

SQSTM1<sup>S351A</sup> overexpressed cells compared to that in WT SQSTM1-overexpressed cells (Figure 5K, S2E). This result indicated that the phosphorylation of SQSTM1 at Ser351 plays an important role in modulating the interaction between SQSTM1 and STING1, which further affects STING1 degradation. Taken together, these data showed that CSNK1A1 accelerates STING1 autophagic degradation by promoting the phosphorylation of SQSTM1 at Ser351.

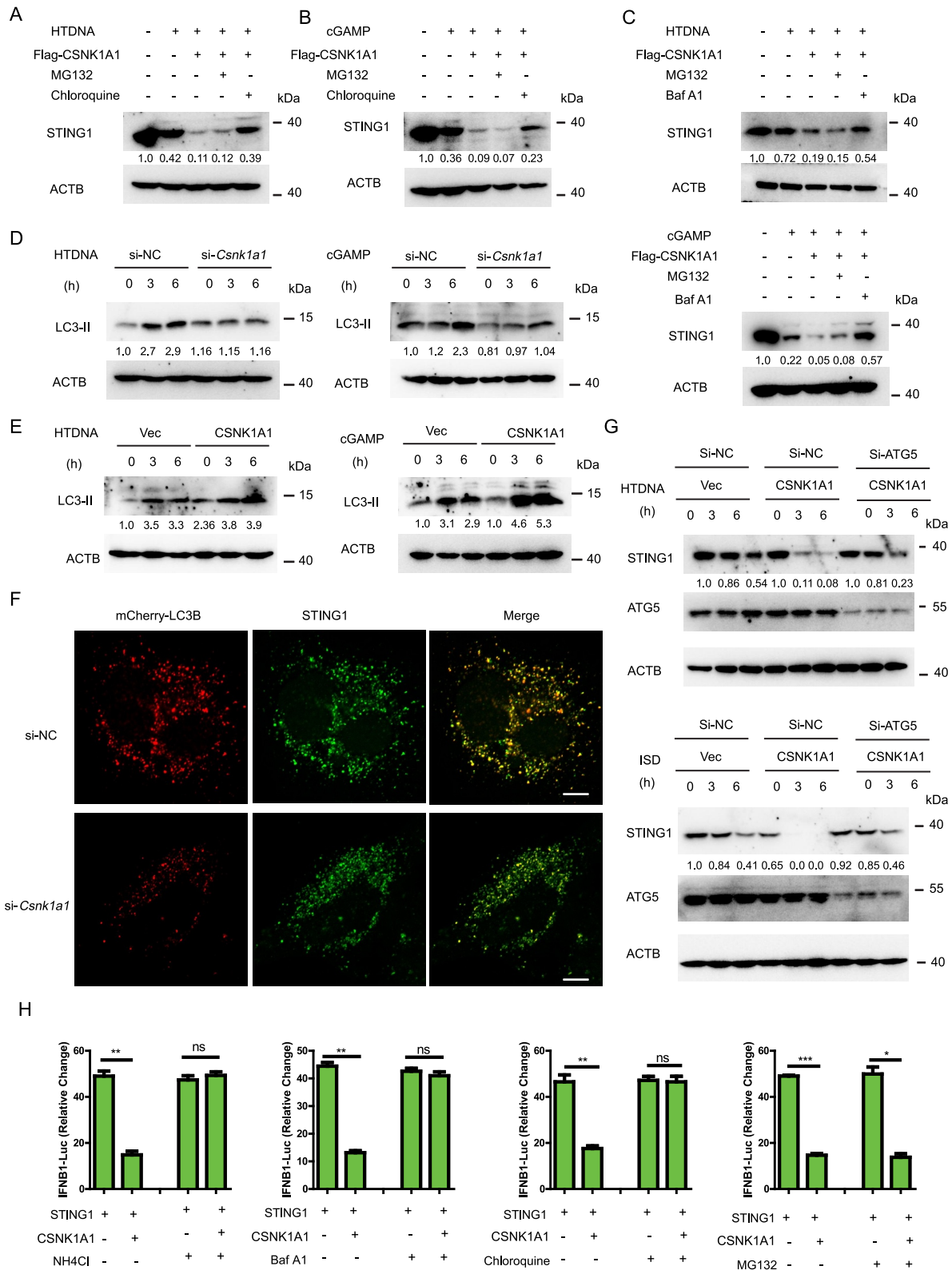
### CSNK1A1 agonist SSTC3 inhibits the CGAS-STING1 signaling by targeting STING1 for degradation

SSTC3 is a selective small-molecule agonist for CSNK1A1 [41]. We next investigated whether SSTC3 could inhibit the CGAS-STING1 signaling. The result showed that SSTC3 treatment significantly impaired the HTDNA or cGAMP induced activation of STING1-IFN-I signaling (Figure 6A). We further carried out RNA-seq experiments to measure molecular changes at the gene expression level in SSTC3-treated and DMSO-treated MEFs after HTDNA stimulation. In line with the impaired IFN-I level, treatment of SSTC3 dramatically downregulated most of the differentially expressed ISGs induced by HTDNA (Figure 6B). Consistently with the RNA-seq data, real-time PCR substantiated a significant decrease in the expression of *Ifnb*, *Cxcl10*, *Ifit1*, and *Rsad2* in SSTC3-treated MEFs after HTDNA stimulation (Figure 6C). Also, IRF3 phosphorylation triggered by HTDNA was attenuated in SSTC3-treatment MEFs compared to that in DMSO-treatment MEFs (Figure 6D). In addition, the expression of ISGs and IRF3 phosphorylation triggered by cGAMP was also markedly decreased in SSTC3-treatment MEFs (Figure 6E,F). Moreover, we found that SSTC3 treatment substantially promoted STING1 degradation after HTDNA or cGAMP stimulation (Figure 6G). Collectively, these data demonstrated that SSTC3 is a potent inhibitor of the CGAS-STING1 signaling by targeting STING1 for degradation.

### Increasing CSNK1A1 activation suppresses aberrant type I IFNs in SLE patients

SLE is a common autoimmune disease characterized by aberrant type I IFN signaling and increased expression of ISGs [42]. Mounting evidence shows that the abnormal activation of the CGAS-STING1 signaling plays a critical pathogenic role in SLE [4,7,8]. Given the important role of CSNK1A1 in suppressing STING1-mediated type I IFN signaling, we wondered whether increasing CSNK1A1 activation could alleviate aberrant type I IFN response in SLE patients. To check this, we isolated PBMCs from the blood samples of SLE patients and transfected them with control empty vectors (Vec) or CSNK1A1 expression plasmids (CSNK1A1) by electroporation. After transfection with CSNK1A1 expression plasmids (CSNK1A1) or its

for western blot analysis of STING1 and ACTB. (I) MEFs transfected control vectors (Vec) or CSNK1A1 mutant expression plasmids (CSNK1A1 mutant) were stimulated with HTDNA (2 µg per well) for 0, 3, 6 h respectively. Then, Cell lysates were collected for western blot analysis of STING1 and ACTB. (J) MEFs transfected control vectors (Vec) or CSNK1A1 mutant expression plasmids (CSNK1A1 mutant) were stimulated with cGAMP (1 µg per well) for 0, 3, 6 h respectively. Then, Cell lysates were collected for western blot analysis of STING1 and ACTB.



**Figure 4.** CSNK1A1 promotes STING1 autophagic degradation. (A) MEFs transfected control vectors (Vec) or CSNK1A1 expression plasmids (CSNK1A1) were stimulated with HTDNA (2  $\mu$ g per well) for 0, 3 h respectively, followed by the treatment of mock, MG132 (10  $\mu$ M), chloroquine (CQ; 50  $\mu$ M). Then, Cell lysates were collected for western blot analysis of STING1 and ACTB. (B) MEFs transfected control vectors (Vec) or CSNK1A1 expression plasmids (CSNK1A1) were stimulated with cGAMP (1  $\mu$ g per well) for 0, 3 h respectively, followed by the treatment of mock, MG132 (10  $\mu$ M), chloroquine (CQ; 50  $\mu$ M). Then, Cell lysates were collected for western blot analysis of STING1 and ACTB. (C) MEFs transfected control vectors (Vec) or CSNK1A1 expression plasmids (CSNK1A1) were stimulated with HTDNA (2  $\mu$ g per well) for 0, 3 h respectively, followed by the treatment of mock, MG132 (10  $\mu$ M), baf A1 (0.2  $\mu$ M). Then, Cell lysates were collected for western blot analysis of STING1 and ACTB. (D) MEFs transfected negative control (NC) or *Csnk1a1* siRnas were stimulated with HTDNA (2  $\mu$ g per well) or cGAMP (1  $\mu$ g per well) for 0, 3, 6 h respectively. Then, Cell lysates were collected for western blot analysis of LC3-II and ACTB. (E) MEFs transfected control vectors (Vec) or CSNK1A1 expression plasmids (CSNK1A1) were stimulated with HTDNA (2  $\mu$ g per well) or cGAMP (1  $\mu$ g per well) for 0, 3, 6 h respectively. Then, Cell lysates were collected for western blot analysis of LC3-II and



control plasmids for 48 h, the levels of CSNK1A1 mRNA were significantly higher in CSNK1A1-treated PBMCs of SLE patients than in Vec-treated PBMCs of SLE patients (Figure 7A). The mRNA levels of *IFNB* and ISGs (*CXCL10*, *ISG15*, *IFIT2*, *IFIT1*) were notably decreased in CSNK1A1-treated PBMCs of SLE patients (Figure 7B–D), suggesting that CSNK1A1 inhibited type I IFN signaling response in the PBMCs of SLE patients. Consistently, the mRNA levels of *IFNB* and ISGs (*CXCL10*, *ISG15*, *IFIT2*, *IFIT1*) were markedly decreased in SSTC3-treated PBMCs of SLE patients (Figure 7E,F). In addition, STING1 degradation was accelerated in SSTC3-treated PBMCs of SLE patients (Figure 7G). Taken together, these data indicated that increasing CSNK1A1 activation through overexpression or using its agonist SSTC3 alleviates aberrant type I IFNs in PBMCs of SLE patients by degrading STING1.

### Pharmacologically activating CSNK1A1 using SSTC3 alleviates autoimmunity in *trex1*<sup>-/-</sup> mice

Having established the critical role of SSTC3 in repressing STING1-mediated type I IFN signaling, we next examined whether pharmacological activation of CSNK1A1 using SSTC3 might alleviate the STING1-mediated autoimmune or autoinflammatory diseases in *trex1*<sup>-/-</sup> mice, which exhibited cytosolic self-DNA induced STING1-dependent IFN-mediated autoimmune disease phenotypes, especially in the heart and other organs. We first examined the effects of SSTC3 on the expression of type I interferon and pro-inflammatory cytokines in *trex1*<sup>-/-</sup> BMDMs. The result showed that SSTC3 inhibited the expression of type I interferon and pro-inflammatory cytokines (*Ifnb*, *Cxcl10*, *Isg15*, *Tnf*, and *Il6*) in *trex1*<sup>-/-</sup> BMDMs (Figure 8A). Moreover, the STING1 protein abundance was decreased in SSTC3-treated *trex1*<sup>-/-</sup> BMDMs compared to DMSO-treated *trex1*<sup>-/-</sup> BMDMs (Figure 8B). To further explore the potential therapeutic role of SSTC3 in *trex1*<sup>-/-</sup> mice, SSTC3 or PBS was injected intraperitoneally for a month into 6-week-old *trex1*<sup>-/-</sup> mice. We found that the administration of the SSTC3 strongly inhibited the expression of *Ifnb*, *Cxcl10*, *Isg15*, *Tnf*, and *Il6* mRNA in the heart, muscle, stomach, and tongue of *trex1*<sup>-/-</sup> mice (Figure 8C). Furthermore, the STING1 protein level was decreased in the heart, spleen, and stomach of SSTC3-treated *trex1*<sup>-/-</sup> mice (Figure 8D). Consistently, histology results showed that the administration of SSTC3 alleviated the autoinflammatory clinical signs in the heart, muscle, tongue and stomach tissues of *trex1*<sup>-/-</sup> mice (Figure 8E). Collectively, these data demonstrated that pharmacologically activating CSNK1A1 using SSTC3 efficiently alleviates autoimmunity in *trex1*<sup>-/-</sup> mice.

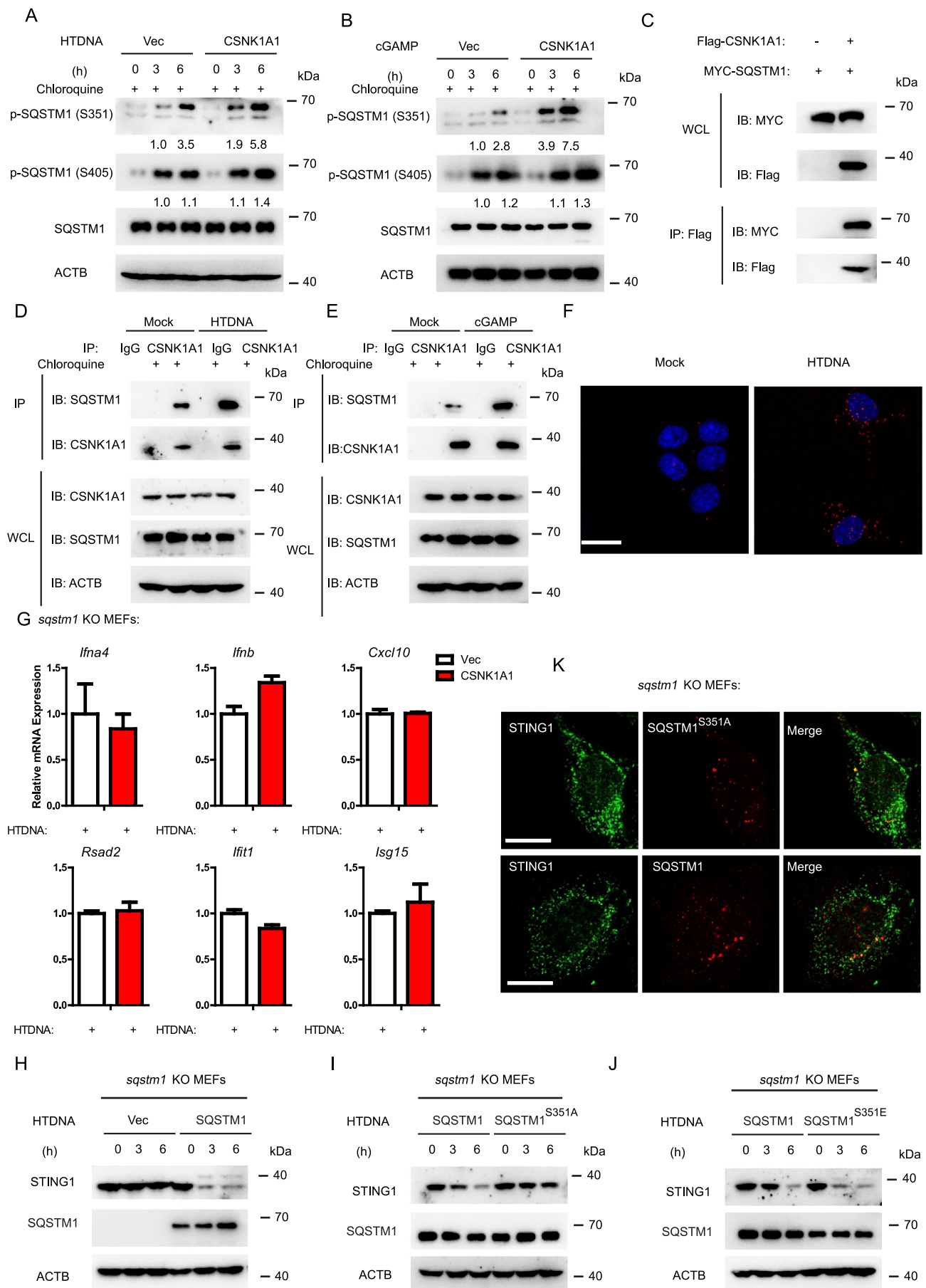
## Discussion

In this study, we reported that CSNK1A1 is a pivotal negative regulator of the CGAS-STING1 signaling. Through promoting STING1 autophagic degradation, CSNK1A1 was essential in preventing the excessive activation of STING1-mediated IFN response (Figure 9). Mechanistically, CSNK1A1 directly interacted with STING1 and promoted the Ser351 phosphorylation of SQSTM1 to degrade STING1 through selective autophagy following the activation of CGAS-STING1 signaling. Furthermore, we found a selective CSNK1A1 agonist SSTC3 repressed the response of the CGAS-STING1 signaling by promoting STING1 autophagic degradation. Importantly, we showed that the overexpression of CSNK1A1 and treatment of SSTC3 both suppressed the production of type I IFNs and ISGs in the PBMCs of SLE patients, and the administration of SSTC3 efficiently attenuated autoimmunity in *trex1*<sup>-/-</sup> mice.

Autophagy is a double-edged sword in innate immunity. On the one hand, it is well known that autophagy functions as a powerful and deeply conserved cellular program induced by the CGAS-STING1 signaling for the host against intracellular bacteria and viruses [43]. On the other hand, autophagy components also negatively regulate CGAS-STING1 signaling to attenuate type I IFN response [44]. The connection between CSNK1A1 and autophagy is also intimate. Previous studies showed that the knockdown of CSNK1A1 leads to nuclear accumulation of FOXO3A and increases the expression of autophagy-related genes, which enhances autophagic flux [45, 46]. In addition, the overexpression of CSNK1A1 significantly induces autophagic flux in NSCLC by the PTEN-AKT-Atg7 axis [31]. Our finding showed that CSNK1A1 promoted the phosphorylation of SQSTM1 at Ser351 to modulate STING1 autophagic degradation, thus providing new insight into the regulatory network regarding STING1 turnover and immune hemostasis in the process of autophagy. Nevertheless, the detailed mechanism regarding the reciprocal regulation between STING1 immunity and the autophagy pathway is still incomplete and requires further investigation. Moreover, although our results demonstrated a strong dependency of CSNK1A1 mediated STING1 degradation on the phosphorylation of SQSTM1 at Ser351, we cannot exclude an intriguing possibility that the degradation of STING1 might also be contributed by CSNK1A1 mediated direct phosphorylation on STING1. More investigations are required to fully dissect the underlying mechanisms of CSNK1A1-mediated STING1 degradation. Besides, whether CSNK1A1 might play a role in regulating type III IFN response in addition to that of type I IFN response also needs further investigations.

SLE is a complex autoimmune disease characterized by high levels of type I IFNs and ISGs, which has been implicated in pathogenesis and disease progression. A recent study has

ACTB. (F) MEFs were transfected indicated siRNA or plasmids and then stimulated with HTDNA for 3 h, then stained with the indicated antibodies before imaging by confocal microscopy. Scale bars: 10  $\mu$ m. (G) MEFs were transfected indicated siRNA or plasmids and then stimulated with HTDNA (2  $\mu$ g per well) or ISD (2  $\mu$ g per well) for 0, 3, 6 h respectively. Then, Cell lysates were collected for western blot analysis of ATG5, STING1 and ACTB. (H) luciferase activity in HEK293 cells transfected with an IFN $\beta$  luciferase reporter, together with STING1 and an empty vector or CSNK1A1-expressing plasmids, followed by the treatment of mock, MG132 (10  $\mu$ M), chloroquine (CQ; 50  $\mu$ M), NH $_4$ Cl (10 mM), or baf A1 (0.2  $\mu$ M). The firefly- and renilla luciferase signals were detected with Dual Glo<sup>®</sup> luciferase assay (Promega). Graphs show the mean  $\pm$  SEM, and the data shown are representative of three independent experiments. \* $p$  < 0.05; \*\* $p$  < 0.01; \*\*\* $p$  < 0.001 (two-tailed t-test).



**Figure 5.** CSNK1A1 accelerates STING1 autophagic degradation by promoting phosphorylation of SQSTM1 at Ser351. (A) MEFs transfected control vectors (Vec) or CSNK1A1 expression plasmids (CSNK1A1) were treated with chloroquine and then stimulated with HTDNA (2  $\mu$ g per well) for 0, 3, 6 h respectively. Then, Cell lysates

reported that a subset of SLE patients have a higher level of cGAMP in the blood samples, and disease activity was tightly correlated with the level of cGAMP [47]. These observations indicated that the CGAS-STING1 pathway could be a critical factor in modulating the production of type I IFN and disease pathogenesis [47]. In addition, it has been reported that STING1-knockout significantly decreased ISG-inducing activity of SLE sera, which indicates that STING1 is an important pathogenic factor of SLE [48]. Blockade of the STING1-IFN-I axis represents a promising therapeutic target for SLE. In this study, we found that CSNK1A1 was a novel regulator to inhibit the production of type I IFNs through preventing excessive STING1 activation. Overexpression of CSNK1A1 or treatment of SSTC3 significantly decreased the production of type I IFNs and ISGs in the PBMCs of SLE patients. Also, pharmacologically activating CSNK1A1 using SSTC3 efficiently attenuated autoimmunity in autoimmune mice model. Hopefully, manipulating CSNK1A1 through SSTC3 might be a potential therapeutic strategy for alleviating STING1-mediated aberrant type I IFNs in autoimmune diseases.

## Materials and methods

### Mice

C57BL/6 WT mice were purchased from the Model Animal Research Center of Nanjing University. The mice were maintained under specific pathogen-free conditions at the Center for New Drug Safety Evaluation and Research, China Pharmaceutical University. The *trex1*<sup>±</sup> mice were kindly gifted from Dr. Tomas Lindahl and Dr. Deborah Barnes (Cancer Research UK, London) and Dr. Nan Yan (University of Texas Southwestern Medical Center). The male and female *trex1*<sup>±</sup> mice were further mated to generate *trex1*<sup>-/-</sup> mice. All genotypes were determined by PCR using T5 Direct PCR Kit (Tsingke, TSE012). All animal experiments were performed in accordance with the National Institutes of Health Guide for the Care and Use of Laboratory Animals. The protocol was approved by the Institutional Animal Care and Use Committee of China Pharmaceutical University and the Institutional Ethics Committee of China Pharmaceutical University (Approval Number 2022-04-002).

### Cell culture

The Human embryonic kidney 293 (HEK293; CRL-1573), HEK293T (CRL-3216) and mouse embryonic fibroblast (MEF; SCRC-1008) cell lines were obtained from the American Type Culture Collection/ATCC. Cell lines were maintained in Dulbecco's modified Eagle's medium (Thermo Fisher Scientific, 11210006; DMEM) containing 10% fetal bovine serum (Thermo Fisher Scientific, 12484028; FBS) under a humidified atmosphere of 5% CO<sub>2</sub> at 37°C. BMDMs were prepared as described previously [9].

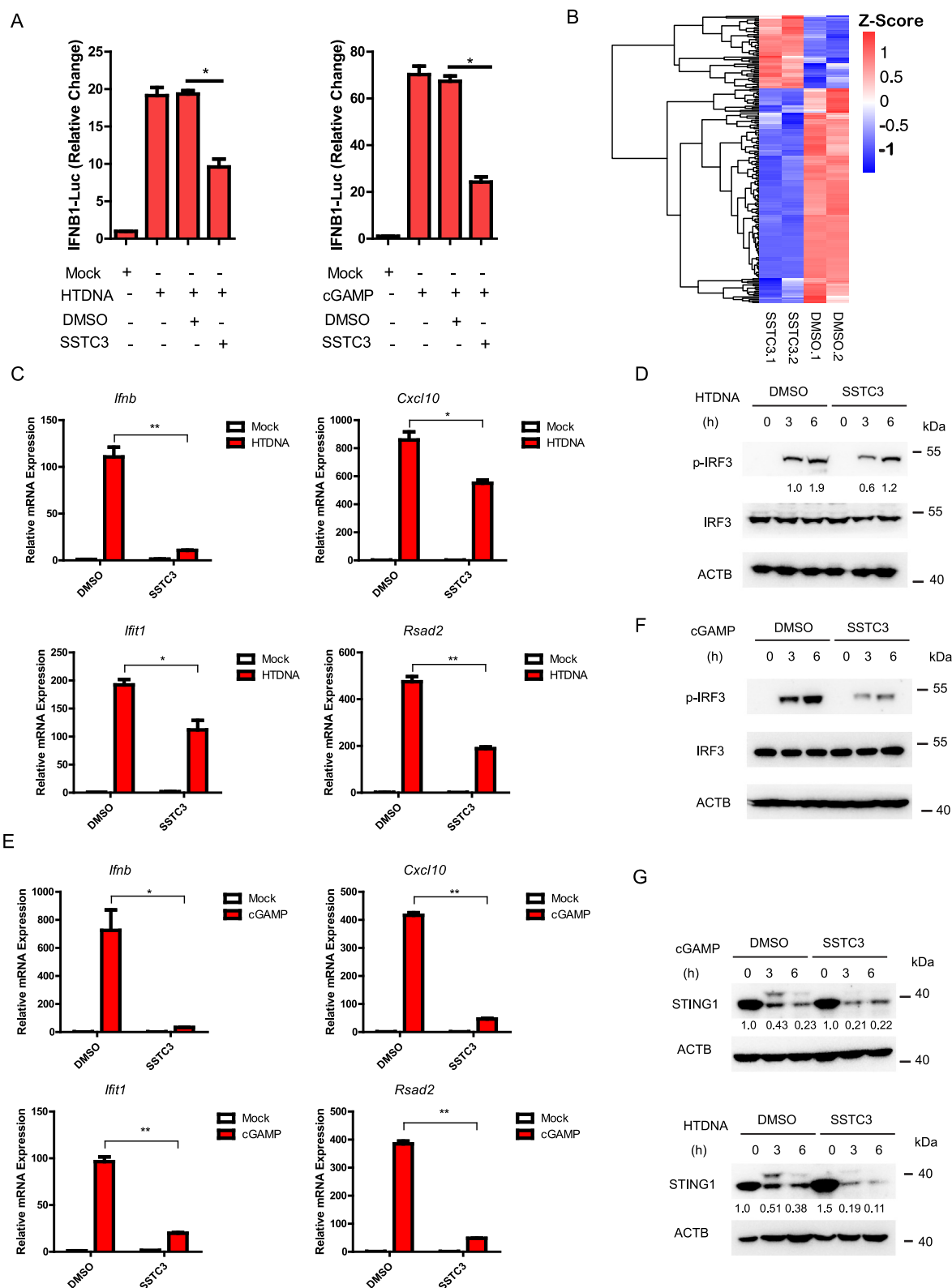
### Isolation of peripheral blood mononuclear cells from SLE patients

Blood was drawn from SLE patients and collected for isolation of PBMCs using Ficoll-plaque (GE Healthcare Lifesciences, 17-1440-02). PBMCs were stored at -80°C. The study was conducted according to the principles of the Declaration of Helsinki and approved by the Institutional Review Board of the Medical ethic committee, The 1st Affiliated Hospital of Nanjing Medical University, in accordance with its guidelines for the protection of human subjects. Specifically, the Institutional Review Board approved the collection of blood samples for this study; the acquisition of samples was conducted in accordance with the guidelines for the protection of human subjects. Written informed consent was obtained from each participant (Approval Number 2020-SR-309).

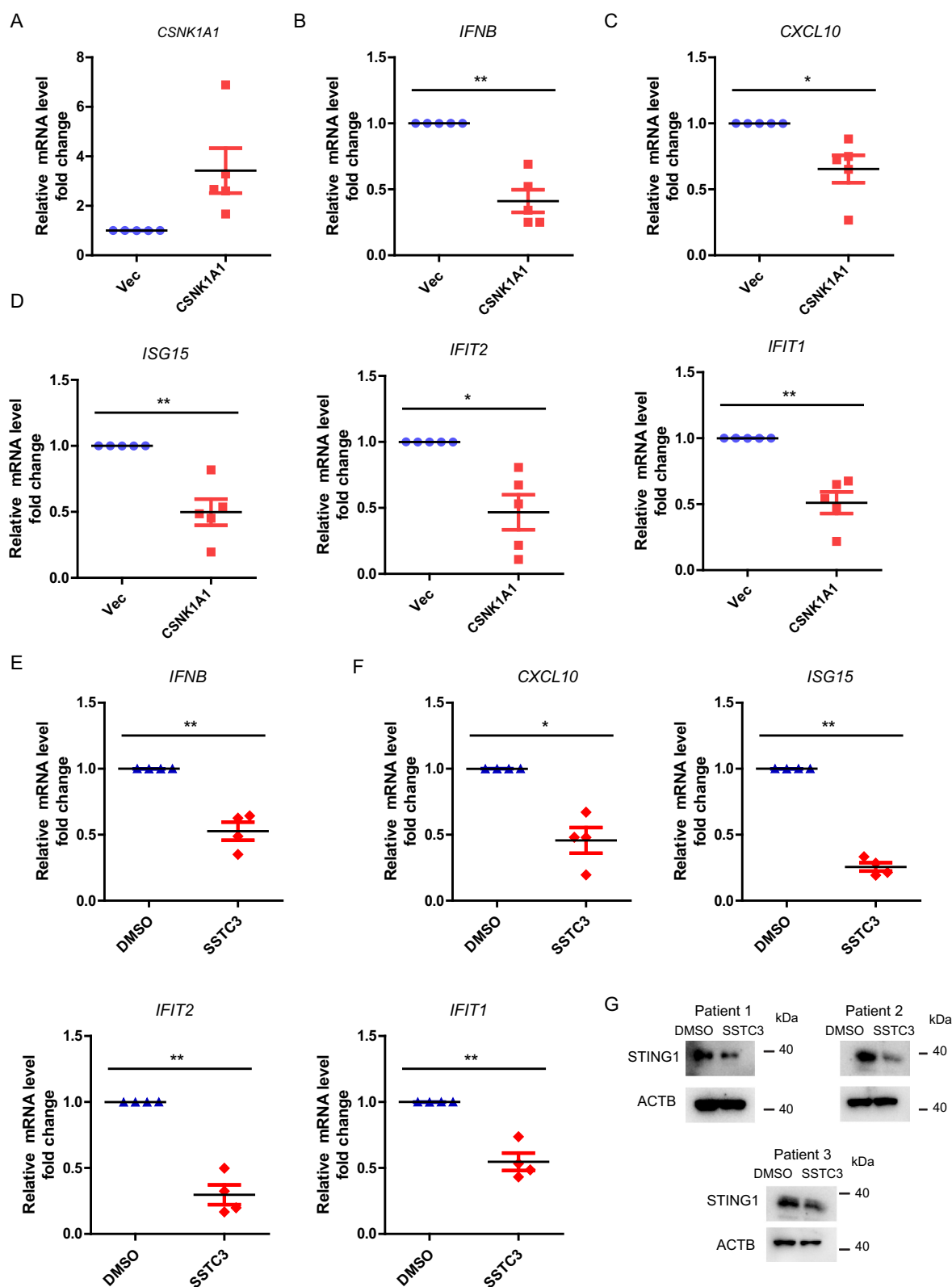
### Antibodies and reagents

The following antibodies were used: anti-CSNK1A1/CK1 (Cell Signaling Technology, 2655S; 1:1000), CSNK1A1 polyclonal antibody (Proteintech, 55192-1-AP), anti-HA (Santa Cruz Biotechnology, sc-7392; Invitrogen, PA1-985; 1:1000), anti-Flag (ABclonal, AE004; SigmaAldrich, F3165; 1:2000), anti-MYC (Santa Cruz Biotechnology, sc-40; 1:2000), anti-STING1 (Cell Signaling Technology, 9664S; R&D Systems, AF6516, MAB7169; 1:1000), anti-phospho-SQSTM1/p62 (Ser349/Ser351; Cell Signaling Technology, 16177S; 1:1000), anti-phospho-SQSTM1/p62 (Ser403/Ser405; Cell Signaling Technology, 39786S; 1:1000), anti-LC3B (Cell Signaling Technology, 3868S; 1:1000), anti-IRF3 (Santa Cruz Biotechnology, sc-9082; Cell Signaling Technology, D83B9;

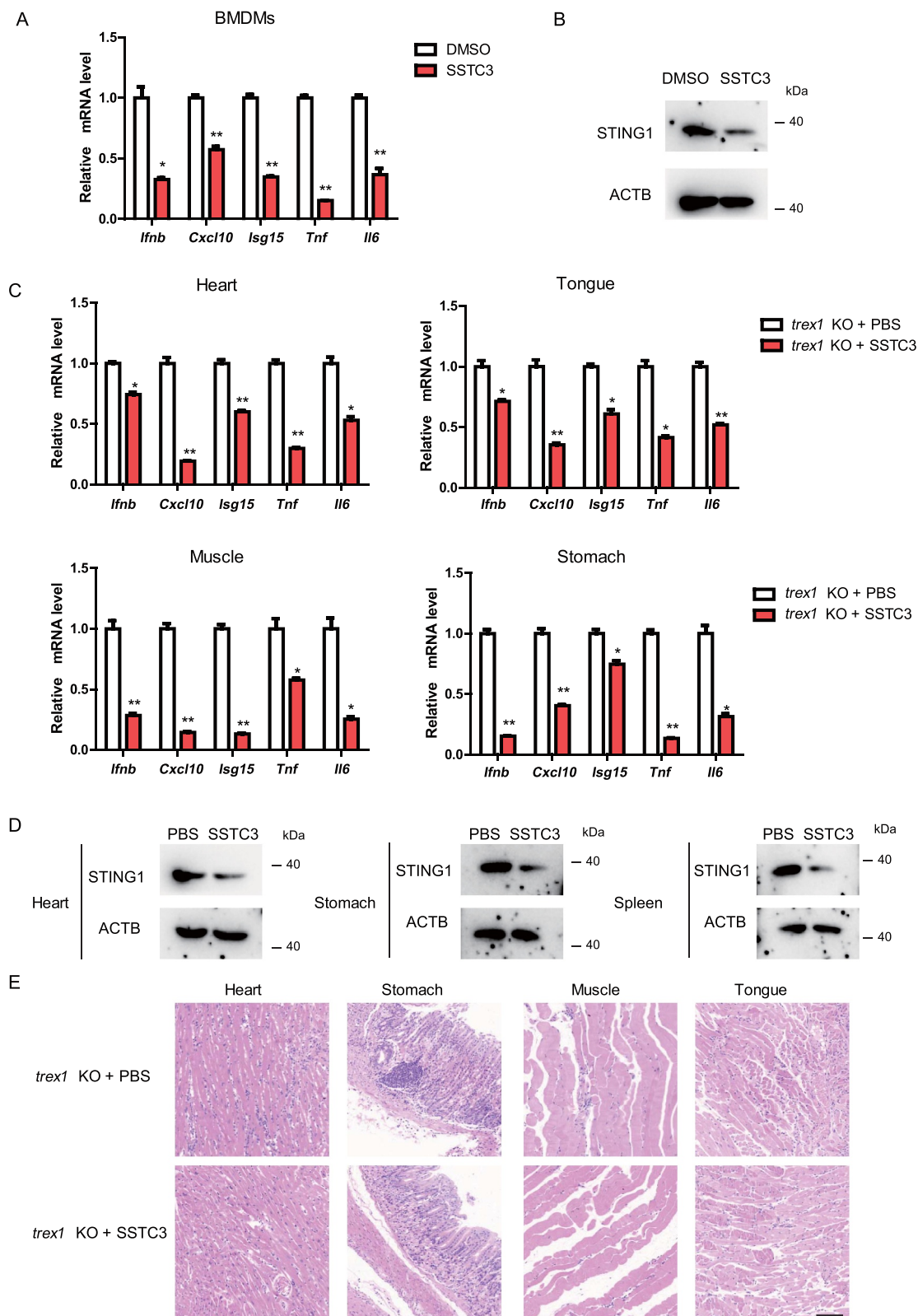
were collected for western blot analysis of p-SQSTM1, SQSTM1 and ACTB. (B) MEFs transfected control vectors (Vec) or CSNK1A1 expression plasmids (CSNK1A1) were treated with chloroquine and then stimulated with cGAMP (1 µg per well) for 0, 3, 6 h respectively. Then, Cell lysates were collected for western blot analysis of p-SQSTM1, SQSTM1 and ACTB. (C) HEK293T cells were transfected with the indicated plasmids. Then, cell lysates were immunoprecipitated with an anti-flag antibody and then immunoblotted with the indicated antibodies. (D) MEFs were treated with chloroquine and then stimulated with HTDNA for 3 h, and the cell lysates were immunoprecipitated with an anti-CSNK1A1 antibody or normal IgG, and then immunoblotted with the indicated antibodies. (E) MEFs were treated with chloroquine and then stimulated with cGAMP for 3 h, and the cell lysates were immunoprecipitated with an anti-CSNK1A1 antibody or normal IgG, and then immunoblotted with the indicated antibodies. (F) MEFs were stimulated with HTDNA for 3 h, then PLA analysis was applied to detect the interaction between CSNK1A1 and SQSTM1. Scale bars: 20 µm. (G) *sqstm1* KO MEFs transfected control vectors (Vec) or CSNK1A1 expression plasmids (CSNK1A1) were stimulated with HTDNA (2 µg per well) for 3 h respectively. Then, the induction of *Irfn1*, *Irfn4*, *Cxcl10*, *Isg15*, *Irf1*, and *Rsad2* mRNAs was measured by real-time PCR. (H) *sqstm1* KO MEFs transfected control vectors (Vec) or SQSTM1 expression plasmids (SQSTM1) were stimulated with HTDNA (2 µg per well) for 0, 3, 6 h respectively. Then, Cell lysates were collected for western blot analysis of STING1, SQSTM1 and ACTB. (I) *sqstm1* KO MEFs transfected SQSTM1 expression plasmids (SQSTM1) or SQSTM1 S351A mutant expression plasmids (SQSTM1<sup>S351A</sup>) were stimulated with HTDNA (2 µg per well) for 0, 3, 6 h respectively. Then, Cell lysates were collected for western blot analysis of STING1, SQSTM1 and ACTB. (J) *sqstm1* KO MEFs transfected SQSTM1 expression plasmids (SQSTM1) or SQSTM1<sup>S351E</sup> mutant expression plasmids (SQSTM1<sup>S351E</sup>) were stimulated with HTDNA (2 µg per well) for 0, 3, 6 h respectively. Then, Cell lysates were collected for western blot analysis of STING1, SQSTM1 and ACTB. (K) SQSTM1 KO MEFs transfected SQSTM1 expression plasmids (SQSTM1) or SQSTM1<sup>S351A</sup> mutant expression plasmids (SQSTM1<sup>S351A</sup>) were stimulated with HTDNA (2 µg per well) for 3 h respectively. Then stained with the indicated antibodies before imaging by confocal microscopy. Scale bars: 20 µm.



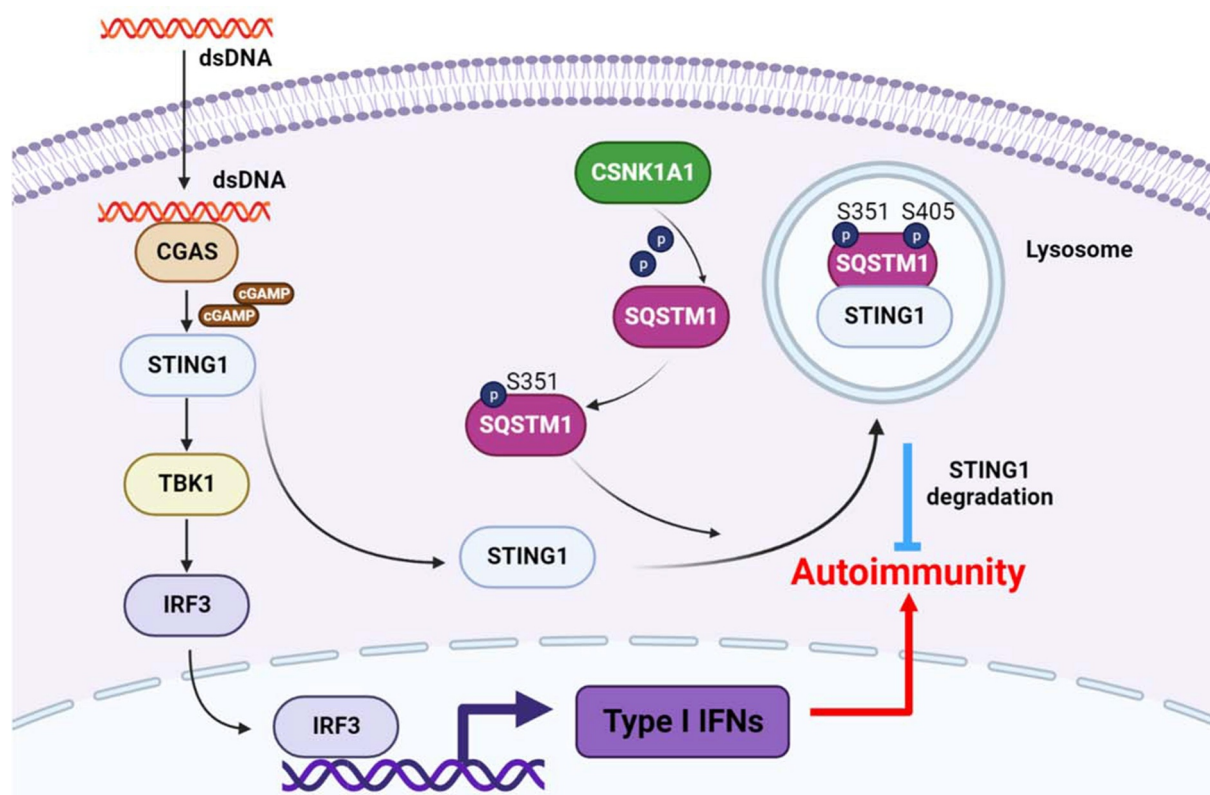
**Figure 6.** SSTC3 is a potent the CGAS-STING1 signaling inhibitor by targeting STING1 for degradation. (A) luciferase activity in HEK293 cells transfected with an IFN $\beta$  luciferase reporter, stimulated with DMSO or SSTC3, activated by HTDNA or cGAMP. The firefly- and renilla luciferase signals were detected with Dual Glo<sup>®</sup> luciferase assay (Promega). (B) the heatmap of expression changes of differentially expressed ISGs between DMSO or SSTC3 treated MEFs stimulated with HTDNA (2  $\mu$ g per well) for 3 h. For each gene, the expression level was normalized (Z-score) across samples. (C) MEFs treated by DMSO or SSTC3 were stimulated with HTDNA (2  $\mu$ g per well) for 3 h. Then, the induction of *Ifnb*, *Cxcl10*, *Ifit1*, and *Rsad2* mRNAs was measured by real-time PCR. (D) MEFs treated by DMSO or SSTC3 were stimulated with HTDNA for 0, 3, 6 h, respectively. Then, cell lysates were collected for western blot analysis of IRF3, IRF3 phosphorylation, and ACTB. (E) MEFs treated by DMSO or SSTC3 were stimulated with cGAMP for 3 h. Then, the induction of *Ifnb*, *Cxcl10*, *Ifit1*, and *Rsad2* mRNAs was measured by real-time PCR. (F) MEFs treated by DMSO or SSTC3 were stimulated with cGAMP for 0, 3, 6 h, respectively. Then, cell lysates were collected for western blot analysis of IRF3, IRF3 phosphorylation, and ACTB. (G) MEFs treated by DMSO or SSTC3 were stimulated with HTDNA or cGAMP for 0, 3, 6 h, respectively. Then, cell lysates were collected for western blot analysis of STING1 and ACTB.



**Figure 7.** CSNK1A1 suppresses aberrant type I IFNs in SLE patients. (A, B, C and D) PBMCs were isolated from the blood samples of SLE patients ( $n = 5$ ). PBMCs were transfected with control vectors (Vec) or CSNK1A1 expression plasmids (CSNK1A1) by electroporation. Then, *CSNK1A1*, *IFNB*, *CXCL10*, *ISG15*, *IFIT2*, and *IFIT1* mRNA were measured by real-time PCR. (E and F) PBMCs were isolated from the blood samples of SLE patients ( $n = 4$ ). PBMCs were treated with DMSO or SSTC3. Then, *IFNB*, *CXCL10*, *ISG15*, *IFIT2*, and *IFIT1* mRNA were measured by real-time PCR. (G) PBMCs were isolated from the blood sample of SLE patients ( $n = 3$ ). PBMCs were treated with DMSO or SSTC3. Then, cell lysates were collected for western blot analysis of STING1 and ACTB.



**Figure 8.** SSTC3-mediated CSNK1A1 activation alleviates autoimmunity in *trex1*<sup>-/-</sup> mice. (A) real-time PCR analysis of *Ifnb*, *Cxcl10*, *Isg15*, *Tnf* and *Il6* mRNA level in BMDMs from *trex1*<sup>-/-</sup> mice treated with DMSO or SSTC3. (B) western blot analysis of STING1 and ACTB in BMDMs from *trex1*<sup>-/-</sup> mice treated with DMSO or SSTC3. (C) real-time PCR analysis of *Ifnb*, *Cxcl10*, *Isg15*, *Tnf* and *Il6* mRNA level in heart, muscle, stomach, and tongue from *trex1*<sup>-/-</sup> mice treated with PBS or SSTC3 (20 mg/kg). (D) western blot analysis of STING1 and ACTB in heart, stomach and spleen from *trex1*<sup>-/-</sup> mice treated with PBS or SSTC3. (E) Hematoxylin and eosin staining of heart, muscle, stomach, and tongue sections isolated from *trex1*<sup>-/-</sup> mice treated with PBS or SSTC3 (scale bar: 100  $\mu$ m).



**Figure 9.** The schematic diagram of the negative regulation of CGAS-STING1 signaling pathway by CSNK1A1.

1:1000), anti-p-IRF3 (Cell Signaling Technology, 4D4G; 1:1000), anti-SQSTM1 (Cell Signaling Technology, 23214S; Genetex, GTX100685; Santa Cruz Biotechnology, sc-48,402; 1:1000), anti-ACTB/ $\beta$ -actin (Cell Signaling Technology, 4967S; 1:1000), normal mouse IgG (Santa Cruz Biotechnology, sc-2025), normal rabbit IgG (Santa Cruz Biotechnology, sc-2027). HTDNA (D6898) was obtained from Sigma-Aldrich. cGAMP (tlrl-nacga23-1) was from Invivogen and was delivered into cultured cells by digitonin (Sigma-Aldrich, 11024-24-1) permeabilization method as previously described [9].

### Real-time PCR

Cell was transfected and stimulated, then cell pellets were collected. Total cellular RNA was isolated using reagent (Invitrogen, 15596018; Accurate Biotechnology Co., Ltd, AG21023, SteadyPure Quick RNA Extraction Kit) according to the manufacturer's instructions, then reverse transcription was performed using a reverse transcription kit (Vazyme, R223-01). The quantification of gene transcripts was performed by real-time PCR using SYBR Green PCR mix (Vazyme, Q331-02/03). All values were normalized to the level of *Gapdh* mRNA using Delta-delta Ct method. The primers used were listed in Table S1.

### Western blot and immunoprecipitation assay

Cell pellets were collected and resuspended in lysis buffer (50 mM Tris-HCl, pH 7.4, 150 mM NaCl, 1 mM EDTA, 0.5%

NP40 [Sigma-Aldrich, NP40], 0.25% Na-deoxycholate [Sigma-Aldrich, D6750], 1 mM  $\text{Na}_3\text{VO}_4$  [Sigma-Aldrich, 450243], 0.1% SDS [Sigma-Aldrich, L3771], 0.1 mM PMSF (phenylmethanesulfonylfluoride or phenylmethylsulfonyl fluoride) [Sigma-Aldrich, PMSF-RO], Roche complete protease inhibitor set [Roche, 04693116001]). The resuspended cell pellet was vortexed for 20 s and then incubated on ice for 20 min, followed by centrifugation. Afterward, supernatants were collected for subsequent western blot analysis. For immunoprecipitation assay, the cell lysate was incubated with appropriate antibodies for 4 h or overnight at 4°C before adding protein A/G agarose beads (Smart Lifesciences, SA032005) for another 2 h. The beads were washed three times with the lysis buffer and eluted with SDS-loading buffer for 5 min.

### Proximity ligation assay

PLA was performed as per manufacturer's instructions (Sigma-Aldrich, DUO82040, DUO92002, DUO92004, DUO92008, DUO82049). The procedure was carried out as described previously [9].

### Plasmids, siRNA oligos, and cell transfection

*Csnk1a1*, *Sting1*, *Cgas*, *Irf3*, *Tbk1*, *Sqstm1*, cDNAs were obtained using standard PCR techniques from thymus cDNA library and subsequently inserted into mammalian expression vectors as indicated. The IRF3 5D was a gift

from Professor John Hiscott (McGill University, Montreal, Quebec, Canada). The siRNA oligos were synthesized by GenePharma: the sequence of *Csnk1a1* siRNA: 5'-GGGCGUCACUGUAAUAAGUTT-3'. Cells were transfected with siRNA oligos using Lipofectamine 3000 (Invitrogen, L3000015) and then incubated for 48 hours before further analysis. The plasmids were introduced into cells using Lipofectamine 3000, and then cells were cultured for 24 h before further analysis. The electroporation of PBMCs was performed using P3 Primary Cell 4D-Nucleofector™ X Kit L (Lonza, V4XP-3024) according to the manufacturer's instructions.

### Dual luciferase reporter assay

Cells were seeded in 12-well plates and transfected with reporter gene plasmids (100 ng) combined with siRNAs and other constructs as indicated. The total amount of DNA was kept constant by supplementing with empty vectors. pTK-Renilla reporter plasmid (2 ng; Promega, E2241) was added to normalize transfection efficiency. Luciferase activity was analyzed with the Dual Luciferase Reporter Assay Kit (Promega, E1910).

### RNA-Seq experiments and analysis

After HTDNA stimulation, total RNA was extracted from control and CSNK1A1-knockdown MEF cells, control and CSNK1A1-overexpression MEF cells using the Trizol reagent (Invitrogen, 15596018) and prepared into cDNA library according to the standard Illumina RNA-seq instruction. The generated cDNA library was sequenced in  $2 \times 150$  bp paired-end layout using Illumina HiSeq2500. Library preparation and sequencing were performed by Novogene (Beijing). To calculate gene expression changes between control and CSNK1A1-knockdown MEFs after HTDNA stimulation, the raw RNA-seq data were preprocessed using Trimmomatic to remove low-quality reads and potential adaptors contamination.

The resulting reads in high-quality were further mapped to the mouse genome (mm10) using HISAT2 with default parameters. The mouse genome (mm10) was downloaded from Ensembl. The gene expression quantification was conducted with feature counts using uniquely mapped reads, based on ensemble mouse gene annotation. The  $\log_2$ -transformed gene expression fold-changes (LFC) and significantly differentially expressed (DE) genes were calculated using edgeR after TMM normalization (FDR < 0.05). The list of known ISGs of mouse was downloaded from. The DE ISGs were obtained by overlapping ISGs with DE genes. The same analysis was performed based on RNA-seq data between control and CSNK1A1-overexpression MEF cells. All original RNA-seq data are deposited in GEO database with accession number: GSE226593.

### Statistical analysis

Except for statistical tests applied to analyze RNA-seq data and downstream functional enrichment, the rest of the statistical analysis was performed using GraphPad Prism 6.0,

Microsoft Excel computer programs. The results are expressed as mean  $\pm$  SEM for experiments conducted at least in triplicates. Student's t-test was used to assess the difference between two groups, and ANOVA with post-hoc Tukey HSD test was used to assess the difference for the analysis of more two groups. A value of  $p < 0.05$  is considered to be statistically significant.

### Acknowledgements

We thank Dr. Ronggui Hu (State Key Laboratory of Molecular Biology, Shanghai Institute of Biochemistry and Cell Biology, Center for Excellence in Molecular Cell Science, Chinese Academy of Sciences) and Dr. Hong Peng (Laboratory of Medical Virology, School of Medicine, Sun Yat-sen University) for sharing the p62 KO MEF cell line. Dr. Yong Yang (The School of Basic Medical Sciences and Clinical Pharmacy, China Pharmaceutical University) and Dr. Xianjing Li (The Institute of Pharmaceutical Sciences, China Pharmaceutical University) for technical support of electroporation. Dr. Wenfeng Tan (Department of Rheumatology, The First Affiliated Hospital of Nanjing Medical University) for collecting SLE patient blood samples. Dr. Chen Wang was supported by the National Key R&D Program of China (2021YFF0702003, 2022YFC2303200), the National Natural Science Foundation of China (31730018, 81672029, 82171751), the Open Project of State Key Laboratory of Natural Medicines (SKLNMZZCX201802), the "Double First-Class" Project of China Pharmaceutical University (CPU2022QZ01). Dr. Haiyang Hu was supported by the National Key R&D Program of China (2022YFC2303200, 2021YFF0702003), the National Science Foundation of Chongqing (CSTB2022NSCQ-MSX1114), Key R&D Project of Jiangsu Province (BE2020725), the "Double First-Class" Project of China Pharmaceutical University (CPU2022QZ01), and the Priority Academic Program Development of Jiangsu Higher Education Institutions (PAPD). Dr. Mingyu Pan was supported by the National Natural Science Foundation of China (82202008), the Natural Science Foundation of Jiangsu Province (BK20221029), the Jiangsu Funding Program for Excellent Postdoctoral Talen (2022ZB307). Dr. Lingxiao Xu was supported by the National Natural Science Foundation of China (82271844), Suqian Sci&Tech Program (KY202201).

### Disclosure statement

No potential conflict of interest was reported by the authors.

### Funding

The work was supported by the National Key R&D Program of China [2021YFF0702003]; the National Key R&D Program of China [2022YFC2303200]; the National Natural Science Foundation of China [82171751]; the Open Project of State Key Laboratory of Natural Medicines [SKLNMZZCX201802]; the National Science Foundation of Chongqing [CSTB2022NSCQ-MSX1114]; Key R&D Project of Jiangsu Province [BE2020725]; the "Double First-Class" Project of China Pharmaceutical University [CPU2022QZ01]; and the Priority Academic Program Development of Jiangsu Higher Education Institutions [PAPD]; the National Natural Science Foundation of China [82202008]; the National Science Foundation of Jiangsu Province [BK20221029]; the Jiangsu Funding Program for Excellent Postdoctoral Talen [2022ZB307]; the National Natural Science Foundation of China [82271844]; Suqian Sci&Tech Program [KY202201].

### Data availability statement

All original RNA-seq data are deposited in the Gene Expression Omnibus database, <https://www.ncbi.nlm.nih.gov/geo> (accession no. GSE226593).



## References

- [1] Cheng Z, Dai T, He X, et al. The interactions between cGAS-STING pathway and pathogens. *Sig Transduct Target Ther.* 2020;5(1):91. doi: [10.1038/s41392-020-0198-7](https://doi.org/10.1038/s41392-020-0198-7)
- [2] Ergun SL, Li L. Structural insights into STING signaling. *Trends Cell Biol.* 2020;30(5):399–407. doi: [10.1016/j.tcb.2020.01.010](https://doi.org/10.1016/j.tcb.2020.01.010)
- [3] Xu Y, Li P, Li K, et al. Pathological mechanisms and crosstalk among different forms of cell death in systemic lupus erythematosus. *J Autoimmun.* 2022;132: 102890. doi: [10.1016/j.jaut.2022.102890](https://doi.org/10.1016/j.jaut.2022.102890)
- [4] Nündel K, Marshak-Rothstein A. The role of nucleic acid sensors and type I IFNs in patient populations and animal models of autoinflammation. *Curr Opin Immunol.* 2019;61:74–79. doi: [10.1016/j.coi.2019.08.003](https://doi.org/10.1016/j.coi.2019.08.003)
- [5] Kumar V. A STING to inflammation and autoimmunity. *J Leukocyte Biol.* 2019;106(1):171–185. doi: [10.1002/JLB.4MIR1018-397RR](https://doi.org/10.1002/JLB.4MIR1018-397RR)
- [6] Motwani M, Pesiridis S, Fitzgerald KA. DNA sensing by the cGAS-STING pathway in health and disease. *Nat Rev Genet.* 2019;20(11):657–674. doi: [10.1038/s41576-019-0151-1](https://doi.org/10.1038/s41576-019-0151-1)
- [7] Yan N. Immune diseases associated with TREX1 and STING dysfunction. *J Interferon Cytokine Res.* 2017;37(5):198–206. doi: [10.1089/jir.2016.0086](https://doi.org/10.1089/jir.2016.0086)
- [8] Hu Y, Chen B, Yang F, et al. Emerging role of the cGAS-STING signaling pathway in autoimmune diseases: biologic function, mechanisms and clinical prospection. *Autoimmun Rev.* 2022;21(9):103155. doi: [10.1016/j.autrev.2022.103155](https://doi.org/10.1016/j.autrev.2022.103155)
- [9] Pan M, Yin Y, Hu T, et al. UXT attenuates the CGAS-STING1 signaling by targeting STING1 for autophagic degradation. *Autophagy.* 2022;19(2):1–17. doi: [10.1080/15548627.2022.2076192](https://doi.org/10.1080/15548627.2022.2076192)
- [10] Zheng W, Xia N, Zhang J, et al. How the innate immune DNA sensing cGAS–STING pathway is involved in autophagy. *Int J Mol Sci.* 2021;22(24):13232. doi: [10.3390/ijms222413232](https://doi.org/10.3390/ijms222413232)
- [11] New J, Thomas SM. Autophagy-dependent secretion: mechanism, factors secreted, and disease implications. *Autophagy.* 2019;15(10):1682–1693. doi: [10.1080/15548627.2019.1596479](https://doi.org/10.1080/15548627.2019.1596479)
- [12] Parzych KR, Klionsky DJ. An overview of autophagy: morphology, mechanism, and regulation. *Antioxid Redox Signal.* 2014;20(3):460–473. doi: [10.1089/ars.2013.5371](https://doi.org/10.1089/ars.2013.5371)
- [13] Levine B, Kroemer G. Biological functions of autophagy genes: a disease perspective. *Cell.* 2019;176(1–2):11–42. doi: [10.1016/j.cell.2018.09.048](https://doi.org/10.1016/j.cell.2018.09.048)
- [14] Byrnes K, Blessinger S, Bailey NT, et al. Therapeutic regulation of autophagy in hepatic metabolism. *Acta Pharm Sin B.* 2022;12(1):33–49. doi: [10.1016/j.apsb.2021.07.021](https://doi.org/10.1016/j.apsb.2021.07.021)
- [15] Pan M, Yin Y, Wang X, et al. Mice deficient in UXT exhibit retinitis pigmentosa-like features via aberrant autophagy activation. *Autophagy.* 2021;17(8):1873–1888. doi: [10.1080/15548627.2020.1796015](https://doi.org/10.1080/15548627.2020.1796015)
- [16] Zhou XJ, Klionsky DJ, Zhang H. Podocytes and autophagy: a potential therapeutic target in lupus nephritis. *Autophagy.* 2019;15(5):908–912. doi: [10.1080/15548627.2019.1580512](https://doi.org/10.1080/15548627.2019.1580512)
- [17] Zhang K, Wang S, Gou H, et al. Crosstalk between autophagy and the cGAS–STING signaling pathway in type I interferon production. *Front Cell Dev Biol.* 2021;9:748485. doi: [10.3389/fcell.2021.748485](https://doi.org/10.3389/fcell.2021.748485)
- [18] Mitzel DN, Lowry V, Shirali AC, et al. Age-enhanced endoplasmic reticulum stress contributes to increased Atg9A inhibition of STING-mediated IFN- $\beta$  production during streptococcus pneumoniae infection. *J Immunol.* 2014;192(9):4273–4283. doi: [10.4049/jimmunol.1303090](https://doi.org/10.4049/jimmunol.1303090)
- [19] Liu D, Wu H, Wang C, et al. STING directly activates autophagy to tune the innate immune response. *Cell Death Differ.* 2019;26(9):1735–1749. doi: [10.1038/s41418-018-0251-z](https://doi.org/10.1038/s41418-018-0251-z)
- [20] Prabakaran T, Bodda C, Krapp C, et al. Attenuation of cGAS-STING signaling is mediated by a p62/SQSTM1-dependent autophagy pathway activated by TBK1. *EMBO J.* 2018;37(8). doi: [10.15252/embj.201797858](https://doi.org/10.15252/embj.201797858)
- [21] Hathaway GM, Traugh JA. Cyclic nucleotide-independent protein kinases from rabbit reticulocytes. Purification of casein kinases. *J Biol Chem.* 1979;254(3):762–768. doi: [10.1016/S0021-9258\(17\)37871-7](https://doi.org/10.1016/S0021-9258(17)37871-7)
- [22] Rowles J, Slaughter C, Moomaw C, et al. Purification of casein kinase I and isolation of cDNAs encoding multiple casein kinase I-like enzymes. *Proc Natl Acad Sci U S A.* 1991;88(21):9548–9552. doi: [10.1073/pnas.88.21.9548](https://doi.org/10.1073/pnas.88.21.9548)
- [23] Amit S, Hatzubai A, Birman Y, et al. Axin-mediated CKI phosphorylation of  $\beta$ -catenin at ser 45: a molecular switch for the wnt pathway. *Genes Dev.* 2002;16(9):1066–1076. doi: [10.1101/gad.230302](https://doi.org/10.1101/gad.230302)
- [24] Liu C, Li Y, Semenov M, et al. Control of  $\beta$ -catenin phosphorylation/degradation by a Dual-kinase mechanism. *Cell.* 2002;108(6):837–847. doi: [10.1016/S0092-8674\(02\)00685-2](https://doi.org/10.1016/S0092-8674(02)00685-2)
- [25] Sinnberg T, Menzel M, Kaesler S, et al. Suppression of casein kinase 1 $\alpha$  in melanoma cells induces a switch in  $\beta$ -catenin signaling to promote metastasis. *Cancer Res.* 2010;70(17):6999–7009. doi: [10.1158/0008-5472.CAN-10-0645](https://doi.org/10.1158/0008-5472.CAN-10-0645)
- [26] Huart AS, MacLaine NJ, Meek DW, et al. CK1 $\alpha$  plays a central role in mediating MDM2 control of p53 and E2F-1 protein stability. *J Biol Chem.* 2009;284(47):32384–32394. doi: [10.1074/jbc.M109.052647](https://doi.org/10.1074/jbc.M109.052647)
- [27] Liu X, Huang Q, Chen L, et al. Tumor-derived CK1 $\alpha$  mutations enhance MDMX inhibition of p53. *Oncogene.* 2020;39(1):176–186. doi: [10.1038/s41388-019-0979-z](https://doi.org/10.1038/s41388-019-0979-z)
- [28] Mbefo MK, Fares M-B, Paleologou K, et al. Parkinson disease mutant E46K enhances  $\alpha$ -synuclein phosphorylation in mammalian cell lines, in yeast, and in vivo. *J Biol Chem.* 2015;290(15):9412–9427. doi: [10.1074/jbc.M114.610774](https://doi.org/10.1074/jbc.M114.610774)
- [29] Shanware NP, Williams LM, Bowler MJ, et al. Non-specific in vivo inhibition of CK1 by the pyridinyl imidazole p38 inhibitors SB 203580 and SB 202190. *BMB Rep.* 2009;42(3):142–147. doi: [10.5483/BMBRep.2009.42.3.142](https://doi.org/10.5483/BMBRep.2009.42.3.142)
- [30] Elyada E, Pribluda A, Goldstein RE, et al. CK1 $\alpha$  ablation highlights a critical role for p53 in invasiveness control. *Nature.* 2011;470(7334):409–413. doi: [10.1038/nature09673](https://doi.org/10.1038/nature09673)
- [31] Cai J, Li R, Xu X, et al. CK1 $\alpha$  suppresses lung tumour growth by stabilizing PTEN and inducing autophagy. *Nat Cell Biol.* 2018;20(4):465–478. doi: [10.1038/s41556-018-0065-8](https://doi.org/10.1038/s41556-018-0065-8)
- [32] Jiang S, Zhang M, Zhang Y, et al. WNT5B governs the phenotype of basal-like breast cancer by activating WNT signaling. *Cell Commun Signal.* 2019;17(1):109. doi: [10.1186/s12964-019-0419-2](https://doi.org/10.1186/s12964-019-0419-2)
- [33] Balka KR, De Nardo D. Molecular and spatial mechanisms governing STING signalling. *FEBS J.* 2020;288(19):5504–5529. doi: [10.1111/febs.15640](https://doi.org/10.1111/febs.15640)
- [34] Hu T, Pan M, Yin Y, et al. The regulatory network of cyclic GMP-AMP synthase-stimulator of interferon genes pathway in viral evasion. *Front Microbiol.* 2021;12:790714. doi: [10.3389/fmicb.2021.790714](https://doi.org/10.3389/fmicb.2021.790714)
- [35] Bustos VH, Marin O, Meggio F, et al. Generation of protein kinase Ck1 $\alpha$  mutants which discriminate between canonical and non-canonical substrates. *Biochem J.* 2005;391(2):417–424. doi: [10.1042/BJ20050717](https://doi.org/10.1042/BJ20050717)
- [36] Hanzl A, Winter GE. Targeted protein degradation: current and future challenges. *Curr Opin Chem Biol.* 2020;56:35–41. doi: [10.1016/j.cbpa.2019.11.012](https://doi.org/10.1016/j.cbpa.2019.11.012)
- [37] Pei J, Wang G, Feng L, et al. Targeting lysosomal degradation pathways: new strategies and techniques for Drug Discovery. *J Med Chem.* 2021;64(7):3493–3507. doi: [10.1021/acs.jmedchem.0c01689](https://doi.org/10.1021/acs.jmedchem.0c01689)
- [38] Schaaf MB, Keulers TG, Vooijs MA, et al. LC3/GABARAP family proteins: autophagy-(un)related functions. *FASEB J.* 2016;30(12):3961–3978. doi: [10.1096/fj.201600698R](https://doi.org/10.1096/fj.201600698R)
- [39] Oh DS, Park JH, Jung HE, et al. Autophagic protein ATG5 controls antiviral immunity via glycolytic reprogramming of dendritic cells against respiratory syncytial virus infection. *Autophagy.* 2021;17(9):2111–2127. doi: [10.1080/15548627.2020.1812218](https://doi.org/10.1080/15548627.2020.1812218)

- [40] Ichimura Y, Waguri S, Sou Y-S, et al. Phosphorylation of p62 activates the Keap1-Nrf2 pathway during selective autophagy. *Mol Cell*. 2013;51(5):618–631. doi: [10.1016/j.molcel.2013.08.003](https://doi.org/10.1016/j.molcel.2013.08.003)
- [41] Li B, Orton D, Neitzel LR, et al., Differential abundance of CK1 $\alpha$  provides selectivity for pharmacological CK1 $\alpha$  activators to target WNT-dependent tumors. *Sci Signal*. 2017;10(485). doi: [10.1126/scisignal.aak9916](https://doi.org/10.1126/scisignal.aak9916)
- [42] Baechler EC, Batliwalla FM, Karypis G, et al. Interferon-inducible gene expression signature in peripheral blood cells of patients with severe lupus. *Proc Natl Acad Sci U S A*. 2003;100(5):2610–2615. doi: [10.1073/pnas.0337679100](https://doi.org/10.1073/pnas.0337679100)
- [43] Choi Y, Bowman JW, Jung JU. Autophagy during viral infection - a double-edged sword. *Nat Rev Microbiol*. 2018;16(6):341–354. doi: [10.1038/s41579-018-0003-6](https://doi.org/10.1038/s41579-018-0003-6)
- [44] Hopfner KP, Hornung V. Molecular mechanisms and cellular functions of cGAS-STING signalling. *Nat Rev Mol Cell Biol*. 2020;21(9):501–521. doi: [10.1038/s41580-020-0244-x](https://doi.org/10.1038/s41580-020-0244-x)
- [45] Szyniarowski P, Corcelle-Termeau E, Farkas T, et al. A comprehensive siRNA screen for kinases that suppress macroautophagy in optimal growth conditions. *Autophagy*. 2011;7(8):892–903. doi: [10.4161/auto.7.8.15770](https://doi.org/10.4161/auto.7.8.15770)
- [46] Zhao J, Brault JJ, Schild A, et al. FoxO3 coordinately activates protein degradation by the autophagic/lysosomal and proteasomal pathways in atrophying muscle cells. *Cell Metab*. 2007;6(6):472–483. doi: [10.1016/j.cmet.2007.11.004](https://doi.org/10.1016/j.cmet.2007.11.004)
- [47] An J, Durcan L, Karr RM, et al. Expression of cyclic GMP-AMP synthase in patients with systemic lupus erythematosus. *Arthritis & Rheumat*. 2017;69(4):800–807. doi: [10.1002/art.40002](https://doi.org/10.1002/art.40002)
- [48] Kato Y, Park J, Takamatsu H, et al. Apoptosis-derived membrane vesicles drive the cGAS-STING pathway and enhance type I IFN production in systemic lupus erythematosus. *Ann Rheum Dis*. 2018;77(10):1507–1515. doi: [10.1136/annrheumdis-2018-212988](https://doi.org/10.1136/annrheumdis-2018-212988)